Balancing water column and sedimentary ²³⁴Th fluxes to quantify coastal marine carbon export

Madeline G. Healey¹, Erin E. Black², Christopher K. Algar¹, Maria Armstrong¹, Stephanie S. Kienast¹

¹Department of Oceanography, Dalhousie University, Halifax, Nova Scotia, Canada

²Department of Earth and Environment, University of Rochester, Rochester, New York, USA

Correspondence to: Madeline G. Healey (mhealey@dal.ca)

Abstract. Quantitative estimates of particulate organic carbon (POC) flux and burial in coastal systems are critical for constraining coastal carbon budgets and understanding their role in regional and global carbon cycling. In this study, POC export fluxes were quantified in the Bedford Basin, a coastal inlet in the Northwest Atlantic, based on measurements of 234 Th/ 238 U disequilibria and the POC: 234 Th ratio on small (1–51 µm) and large (> 51 µm) particles. These water column export fluxes were compared to sediment accumulation fluxes of 234 Th and POC to refine the carbon budget in the Bedford Basin. The coupled water column-surficial sediment sampling approach, which is relatively new, was applied quasi-seasonally throughout 2021–2024, including for the first time in boreal winter. Total 234 Th activities reveal persistent deficits with respect to 238 U throughout the water column, likely due to extensive particle scavenging, which is also indicated by high 234 Th activities on particles. Here, we find that the removal of 234 Th in the water column is typically balanced, within uncertainties, by the inventory of excess 234 Th in underlying marine sediments. This finding reveals that on the timescale of ~100 days, the 234 Th budget in the Bedford Basin is in balance, and no major particle loss is occurring. Using the POC: 234 Th ratio on sinking particles and integrated 234 Th water column fluxes, we report a mean (\pm s.d.) depositional flux of 20 ± 14 mmol C m $^{-2}$ d $^{-1}$ (range 3.6 to 44.5 mmol C m $^{-2}$ d $^{-1}$) to the seafloor. This mean flux translates to an annual molar flux of 7.3 ± 5.1 mol C m $^{-2}$ yr $^{-1}$, within a factor of 2 of model estimates and previous sediment trap results at this site. Our findings contribute to ongoing research efforts in the Bedford Basin, and aid in the evaluation of coastal regions in local carbon budgets.

1. Introduction

5

10

15

20

25

30

35

Coastal and continental shelf zones represent only ~ 7 –10% of the global ocean surface area but host up to 30% of global marine primary production (Muller-Karger et al., 2005) and are important for the long-term burial of organic matter. Coastal areas are dynamic transition zones between land and ocean, where biogeochemical processes modify carbon cycling. In turn, these processes influence air-sea carbon dioxide (CO₂) exchanges and thus exert a significant control on regional and global carbon cycles. A series of biologically mediated processes referred to as the biological carbon pump (BCP) are important in coregulating atmospheric CO₂ concentrations. In the sunlit surface ocean, primary producers photosynthesize inorganic CO₂ into particulate organic carbon (POC) at a rate of ~ 50 Pg C yr⁻¹ (Longhurst et al., 1995). A portion of this POC leaves the surface ocean and sinks to depth, whereby a small fraction ends up sequestered in marine sediments. The traditional method of estimating sinking POC fluxes is based on sediment traps, which suffer from conveyance issues and hydrodynamic biases (Butman, 1989). Additionally, living organisms ("swimmers") can enter traps and bias particle flux estimates, an issue which is more severe in the shallow waters characterizing coastal and shelf areas compared to the open ocean (Buesseler et al., 2007). Given these methodological constraints, the confluence of terrestrial and marine carbon sources, and temporal and spatial heterogeneity, the processes controlling carbon cycling in coastal and shelf regions remain elusive.

First proposed by Bhat et al. (1969), the disequilibrium between the naturally occurring radioisotopes thorium-234 (²³⁴Th, t_{1/2} = 24.1 d) and uranium-238 (²³⁸U, t_{1/2} = 4.47 x 10⁹ yr) is commonly measured to quantify sinking fluxes of carbon and other elements in the ocean. In shallow regions, the removal of ²³⁴Th from the water column results in an excess of ²³⁴Th (²³⁴Th_{xs}) on the seafloor in marine sediments (Aller and Cochran, 1976), offering a unique opportunity to explore one-dimensional (1D) particle dynamics and export. A recent global oceanic compilation identified 223 studies that applied the ²³⁴Th/²³⁸U disequilibrium method, encompassing a total of 1981 unique stations (Ceballos-Romero et al., 2022). However, in nearshore coastal settings, defined here as within 5 nautical miles (nm) of the coast, there are comparatively fewer studies. Of the 1981 unique stations that have been sampled for ²³⁴Th (Ceballos-Romero et al., 2022), only 1.4 % are in nearshore coastal settings. Importantly, only few of the 223 studies make coupled, quasi-simultaneous measurements of the ²³⁴Th deficit in the water column and the expected excess of ²³⁴Th in surficial sediments (Cochran et al., 1995; Charette et al., 2001; Black et al., 2023; Lepore et al., 2007; Turnewitsch and Springer, 2001). By using this approach, detailed insights into carbon export can be made that aid in carbon budget evaluations. This study applies the coupled water column-sediment approach to evaluate both ²³⁴Th and POC sinking fluxes and their respective sediment accumulation fluxes in the Bedford Basin, a coastal fjord in the Northwest Atlantic Ocean.

2. Methods

40

45

50

55

60

65

70

2.1. Study site

The Bedford Basin (BB; 44.6955° N, 63.6330° W; Fig. 1) is a 17 km², semi-enclosed fjord in Nova Scotia, Canada, and forms the northwestern part of the Halifax Harbour. The basin has a volume of 5.6 x 108 m³ (Burt et al., 2013) and a maximum depth of 70 m. It is connected to the inner Halifax Harbour via a 20 m deep sill and to the open Atlantic Ocean by a 10 km long channel that is less than 400 m wide at its narrowest point (Li and Dickie, 2001). Runoff from the Sackville River (1.5 × 10⁸ m³ yr⁻¹, Kepkay et al., 1997) and surrounding areas is discharged into the basin, creating a two-layer estuarine circulation – a fresher top layer and a denser bottom layer from the shelf water intruding from the entrance of the Halifax Harbour. The hydrography of the basin is characterized by annual cycles of winter mixing and summer stratification. Stratification is established in the spring (April–May) and persists into the fall and winter (November–February). In most years, the water column fully mixes during the late winter (mid-February to mid-March). Seasonal hypoxia occurs in the deeper basin during the fall, but re-oxygenation takes place during late winter mixing. In spring, a phytoplankton bloom typically occurs as surface stratification increases. Chlorophyll-a (chl-a) concentrations in surface waters (1–10 m) typically range from ~3–10 mg m⁻³. Spring blooms typically range from ~7–28 mg m⁻³ (Fisheries and Oceans Canada, 2025), while extreme short-lived events can exceed 100 mg m⁻³ (Li and Dickie, 2001). Occasional intrusions of dense Scotian Shelf water can replenish either the bottom or mid-depth waters (Shi and Wallace, 2018; Haas et al., 2021). The Bedford Basin Monitoring Program (BBMP), established by the Bedford Institute of Oceanography (BIO) has conducted weekly measurements of water properties since 1992. Despite a large array of oceanographic variables that are frequently sampled by BBMP and other emerging research initiatives (Fennel et al., 2023; Burt et al., 2024), limited information exists on POC export and burial in this important urban coastal region.

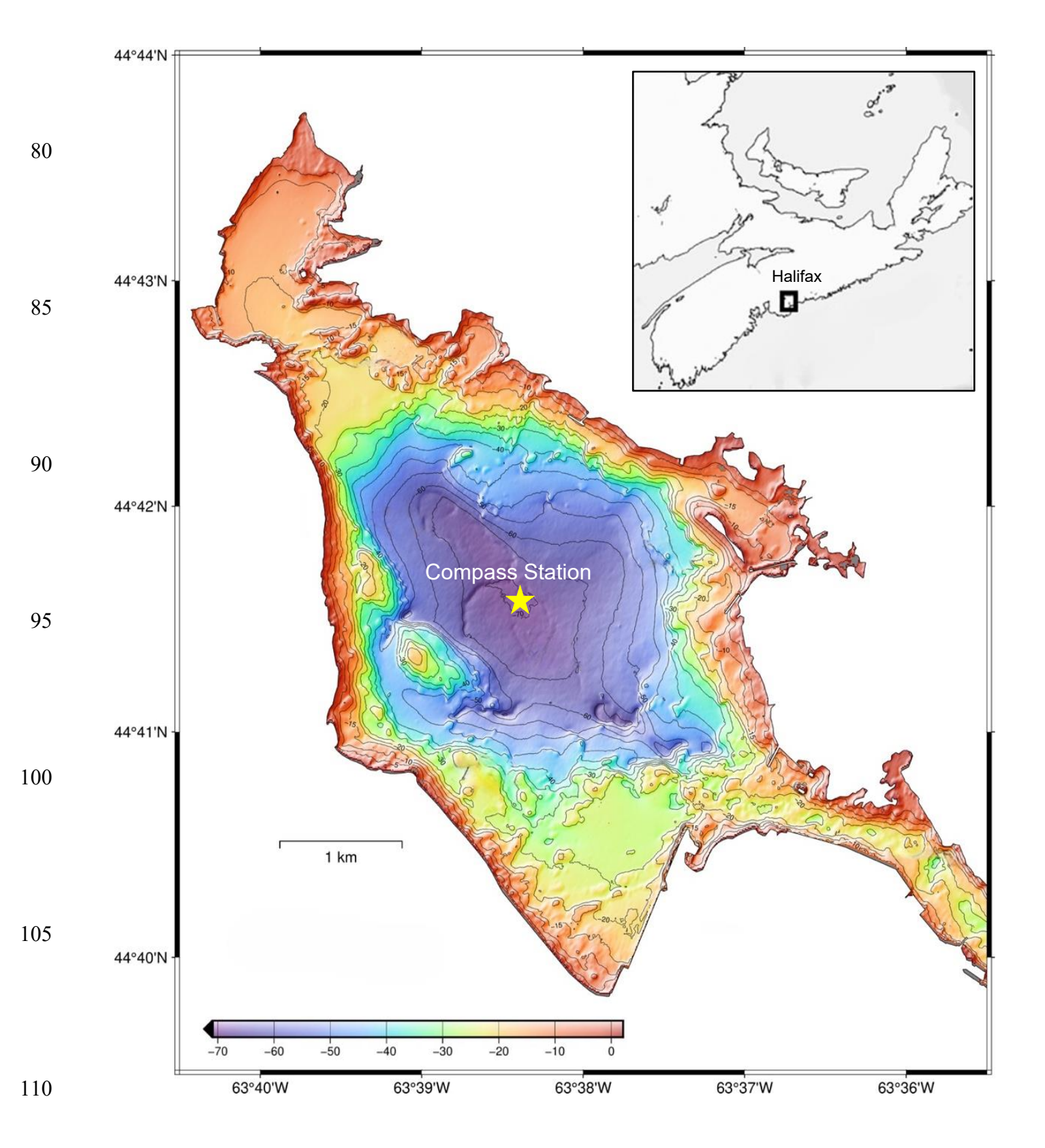


Figure 1: A bathymetric map of the Bedford Basin (GEBCO Gridded Bathymetry Data). Compass Buoy Station (70 m), the main sampling location, is represented by the yellow star. The inset map (upper right corner) shows the relative position of the Bedford Basin in Halifax, Nova Scotia, Atlantic Canada.

2.2. Hydrographic properties

120

125

130

135

140

145

150

155

Weekly monitoring at the Compass Buoy Station in the centre of the Bedford Basin provides temperature, salinity, oxygen, and chl-a concentrations (BBMP, Seabird CTD SBE-25). To capture the mean conditions near the basin floor, we derived mean values for temperature, salinity, and oxygen between 60 m water depth and the bottom (or the deepest available measurement). We then calculated the anomalies between consecutive profiles, resulting in a time series of anomalies that reflects changes from week to week in each variable in the deep basin (Fig. 2d).

2.3. Total ²³⁴Th and ²³⁸U activities in seawater

Total (dissolved + particulate) ²³⁴Th (²³⁴Th_{tot}) was measured six times at the Compass Station between 2021–2024. Water column samples were collected using 10 L Niskin bottles at 9 discrete depths. From each bottle, a 2 L subsample of unfiltered seawater was taken, spiked with a ²³⁰Th yield tracer, and processed according to the MnO₂ co-precipitation technique (Pike et al., 2005). Following co-precipitation, samples were filtered onto quartz fiber filters (QMA, 25 mm diameter, 1 µm nominal pore) following Cai et al. (2006). After filtration, filters were dried (55° C), mounted on sample holders, covered with MylarTM film (1 layer) and aluminium foil (2 layers), and their beta emissions were measured on low-level beta GM multi-counters (Risø National Laboratory, Denmark). Samples were counted until the error was typically < 3 %. After > 120 days from collection (i.e., after 5-6 half-lives of ²³⁴Th had passed), samples were recounted to determine the non ²³⁴Th beta activity stemming from other radionuclides included in the precipitate, which was subtracted from the first count. After final counting was completed, the chemical recovery of ²³⁰Th was determined by inductively coupled plasma mass spectrometry (ICP-MS) as outlined in Clevenger et al. (2021), yielding a mean recovery of 85 ± 12 % (n = 63). The net counting rate was corrected for ²³⁴Th decay and ingrowth, counting efficiency, and chemical recovery. The uncertainties in the ²³⁴Th_{tot} activities are determined from counting statistics and the propagation of errors in relation to sample processing, including mass and volume measurements, and ICP-MS recovery analysis. The parent ²³⁸U activity is derived from salinity following the relationship given by Owens et al. (2011), (Eq. 1).

$$^{238}U (\pm 0.047 \text{ dpm } L^{-1}) = (0.0786 \pm 0.045) \times Salinity = (0.315 \pm 0.158)$$
 (1)

Additional work conducted on 15 January 2025 measured salinity (PSU) and dissolved 238 U activities at multiple locations and depths in the Bedford Basin across a salinity range of 0.1–31.2 (n = 26) and yielded a strong correlation with salinity (R² = 0.99). At the Compass Station specifically, measured dissolved 238 U activities (at 1, 6 and 50 m) were within 1% of the activities predicted by the U-Salinity relationship, confirming the applicability of the Owens et al. (2011) relationship at this site.

Seawater ²³⁴Th activities are used to calculate cumulative water column ²³⁴Th fluxes (dpm m⁻² d⁻¹) as follows:

$$Flux_{Th@z} = \int_{0}^{z} (\lambda_{Th}(^{238}U - ^{234}Th) + w(\frac{\partial^{234}Th}{\partial z}) - u(\frac{\partial^{234}Th}{\partial z}) - v(\frac{\partial^{234}Th}{\partial z})) dz$$
 (2)

Here, 234 Th is 234 Th_{tot} activity (dpm L^{-1}), 238 U is the salinity derived 238 U activity (dpm L^{-1} ; Owens et al., 2011), λ_{Th} is the decay constant of 234 Th (0.0288 d⁻¹), w is the upwelling velocity, u is the zonal velocity, v is the meridional velocity, and the ∂ terms are the vertical (∂z), west to east (∂x), and south to north (∂y) gradients. Applying the 1D steady state model, Eq. 2 can be simplified to:

$$Flux_{Th@z} = \int_0^z (\lambda_{Th}(^{238}U - ^{234}Th) dz$$
 (3)

Given the temporal resolution of this study, and the fact that ²³⁴Th profiles were not measured during consecutive weeks—months but rather on a quasi-seasonal scale, the use of a non-steady-state model for ²³⁴Th flux is not feasible, and we apply the steady state condition. The validity of the 1D steady-state assumption is discussed further in Section 4.3. The uncertainties of the flux are the propagated measurement error.

2.4. Particulate ²³⁴Th and POC in seawater

Size fractionated particulate ²³⁴Th samples (²³⁴Th_p) were collected by in-situ pumping of ~ 30 L at 3 depths (~20, 40, 60 m) using large volume pumps (McLane LaboratoriesTM). Filter heads were equipped with a 51 μm pore size Nitex filter above a 1 μm pore size QMA filter (pre-combusted). The large particle material (> 51 μm) captured on the Nitex screens was carefully rinsed onto QMA filters (1 μm pore size, 25 mm diameter, pre-combusted) using 0.2 μm filtered and ultraviolet (UV) treated seawater. The small particulate material (1–51 μm) captured on the QMA filter was subsampled by cutting out a 25 mm diameter punch. After drying (55 °C) all particulate samples were mounted onto sample holders and analyzed on beta counters (see above). Following the second counting, particulate samples were prepared for POC measurement by fumigation under HCl vapor for 6 h inside a glass desiccator to remove the carbonate phase. Samples were dried at 50 °C and packed into tin cups and then measured on an Elemental Analyzer (Elementar MicroCube & Isoprime 100). For each pump cast, an additional filter head was attached to the deepest pump to obtain a seawater process blank ("dipped blank"; Lam et al., 2015). The dipped blanks were exposed to seawater for the same amount of time and processed as regular samples. Dipped blank filters were used as process blanks for blank subtraction, detection limit determination, and uncertainty calculations. The POC flux can be calculated with either (a) the POC:²³⁴Th ratio on small particles, or (b) the POC:²³⁴Th ratio on large particles using Eq. 4. The fluxes reported using either (a) or (b) represent two alternative approaches to estimating flux, and should not be considered additive, but rather complementary perspectives on export.

180
$$POC Flux = Flux_{Th @ z} \times \left(\frac{POC}{^{234}Th}\right)_{(a),(b)}$$
 (4)

To investigate the role of resuspension in this study and in the Bedford Basin as a whole, the residual beta activity of particulate 234 Th (Ra_{P234}) was analyzed. Ra_{P234} is a novel resuspension proxy (Lin et al., 2016) and has previously been applied to investigate particle dynamics in coastal sites. Briefly, the Ra_{P234} signal comes from "supported" radionuclides bound to particle components like biogenic or lithogenic materials. Terrigenous particles retain radionuclides such as 234 Th (from 238 U decay) and 212 Bi (from 228 Th decay), contributing to β counting due to their long half-lives. In contrast, "unsupported" 234 Th is adsorbed in the water column and is the focus of this (and other studies) using the 234 Th/ 238 U method to quantify carbon fluxes. The supported Ra_{P234} signal indicates sediment resuspension, potentially biasing particle flux measurements. Ra_{P234} was obtained from the second counting rates of 234 Th_p after 5-6 half-lives (> 120 d) passed, and calculated as:

$$RA_{P234} = \left(\frac{n_{p2} - n_0}{\epsilon V}\right) \tag{5}$$

Where n_{p2} is the second β counting rate of 234 Th_p (mean 0.3 ± 0.07 counts per minute (cpm)), n_0 is the blank mean (0.24 ± 0.02 cpm), ϵ is the detector efficiency (0.38), and V is volume of seawater pumped (L). The detection limit is defined here as two times the standard deviation of the blank and corresponds to 128.2 dpm m⁻³.

2.5. Excess ²³⁴Th inventories in seafloor sediments

195

200

205

210

215

220

225

230

For the measurement of ²³⁴Th in the sediment, a KC DenmarkTM Multicorer was deployed at the Compass Station following water column sampling. Sediments were processed either the same day of retrieval or stored at (4° C) for 24–48 h prior to processing. Cores were sliced in 0.5–1 cm thick sections and then dried at 55° C for approximately 24 h. After this period, they were weighed and returned to the oven and reweighed at regular intervals until a constant weight was achieved. To correct for residual salt content, salt contribution from porewater was estimated from the salinity of the overlying water and subtracted from the measured dry weight. Once dry, sediments were manually homogenized and weighed into a petri-dish. Analyses of sedimentary ²³⁴Th and ²³⁸U activities were carried out by non-destructive gamma counting on High-Purity Germanium (HPGe) detectors (Dartmouth College, USA) with ~ 15 g of sediment. The raw ²³⁴Th activities (at 63.3 keV) in sediments were decay corrected to time of collection. Unsupported or 'excess' ²³⁴Th (²³⁴Th_{xs,0}) is ²³⁴Th that is not in secular equilibrium with the ²³⁸U parent present in the uppermost sediments, presumably because it was supplied by settling particles. Supported ²³⁴Th, in equilibrium with ²³⁸U present in the sediment, is identified at the core depth below which no further decrease in ²³⁴Th activities is observed ("Equilibrium Depth"; EQ). The supported activity is subtracted from the total activity to derive ²³⁴Th_{xs,0} (Eq. 6).

$$^{234}Th_{xs,0} = (Decay\ Corrected \quad ^{234}Th) - (Supported \quad ^{234}Th)\ (dpm\ g^{-1}) \tag{6}$$

Sediment inventories of 234 Th_{xs,0} were multiplied by dry bulk density, and the decay constant of 234 Th (0.0288 d⁻¹) and integrated from 0 to the EQ to derive the sediment accumulation flux of 234 Th_{xs,0} on the sea floor (Eq. 7).

Finally, to derive the sediment accumulation flux of POC, following Eq. 4, the 234 Th sediment accumulation flux (Eq. 7) are multiplied by the water column (a) small and (b) large particle POC: 234 Th ratios measured at 65 m, the depth which represents particles that are about to settle on the seafloor (70 m). The POC: 234 Th ratios directly measured in the sediment are not used as 234 Th decays away faster than organic carbon is respired in sediments. Total organic carbon (TOC) content in sediments was measured on an Elemental Analyzer (Elementar MicroCube) at Dalhousie University. Previous work on Bedford Basin sediments compared acid-fumigated and non-acid fumigated samples and found that the mean carbon content did not differ between the acid fumigated (5.5 % \pm 0.5 %, n=29) and non-acid fumigated (5.7 % \pm 0.8 %, n=39) samples (Black et al., 2023). This published finding is consistent with additional unpublished measurements that were made over the years at Dalhousie University. Collectively, the data imply that most of the sedimentary carbon is organic in nature, and thus acid fumigation was not done here.

Sediment Accumulation Flux
$$^{234}Th = \int_0^{EQ} \lambda Th \left(^{234}Th - ^{238}U\right) dz = \int_0^{EQ} \lambda \left(^{234}Th_{xs,0}\right) dz$$
 (7)

3. Results

3.1. Hydrography of Bedford Basin in 2021 - 2024

Hydrographic conditions in the Bedford Basin (2021–2024) generally align with long term trends (Li and Harrison, 2008; Haas et al., 2021). Winter and spring surface cooling reduce summer stratification and drive vertical convection (Fig. 2a). However, 2021 saw higher sea surface temperatures (SSTs), leading to stronger stratification (Rakshit et al., 2023), and a lack of shelf water intrusions (Fig. 2e). That year, bottom waters experienced a six-week oxygen minimum, in contrast with records from 2014–2020 when mixing and intrusions increased dissolved oxygen in the Bedford Basin (Haas et al., 2021). The absence of winter mixing in 2021 may be linked to warmer air temperatures from January–March 2021 (- 0.2 °C), compared to the long-term mean (Environment and Climate Change Canada, 2018) at this site (- 1.5 °C). A spring phytoplankton bloom followed the cessation of winter mixing (Fig. 2d), with chlorophyll maxima at 5–10 m depth. The 2021 bloom, as denoted by chl-a signals, was relatively weak, (11.1 mg m⁻³) compared to stronger blooms observed in 2022 and 2023. The largest spring bloom sampled in this study occurred in 2023 (34.9 mg m⁻³). Deep chl-a signals are observed down to 70 m depth in some sampling events (May 2023). A secondary fall bloom occasionally occurred, including one in late summer 2021 (15.4 mg m⁻³ chl-a). Two intrusion events were observed throughout 2021–2024 (Nov 2022, January 2024; Fig. 2e).

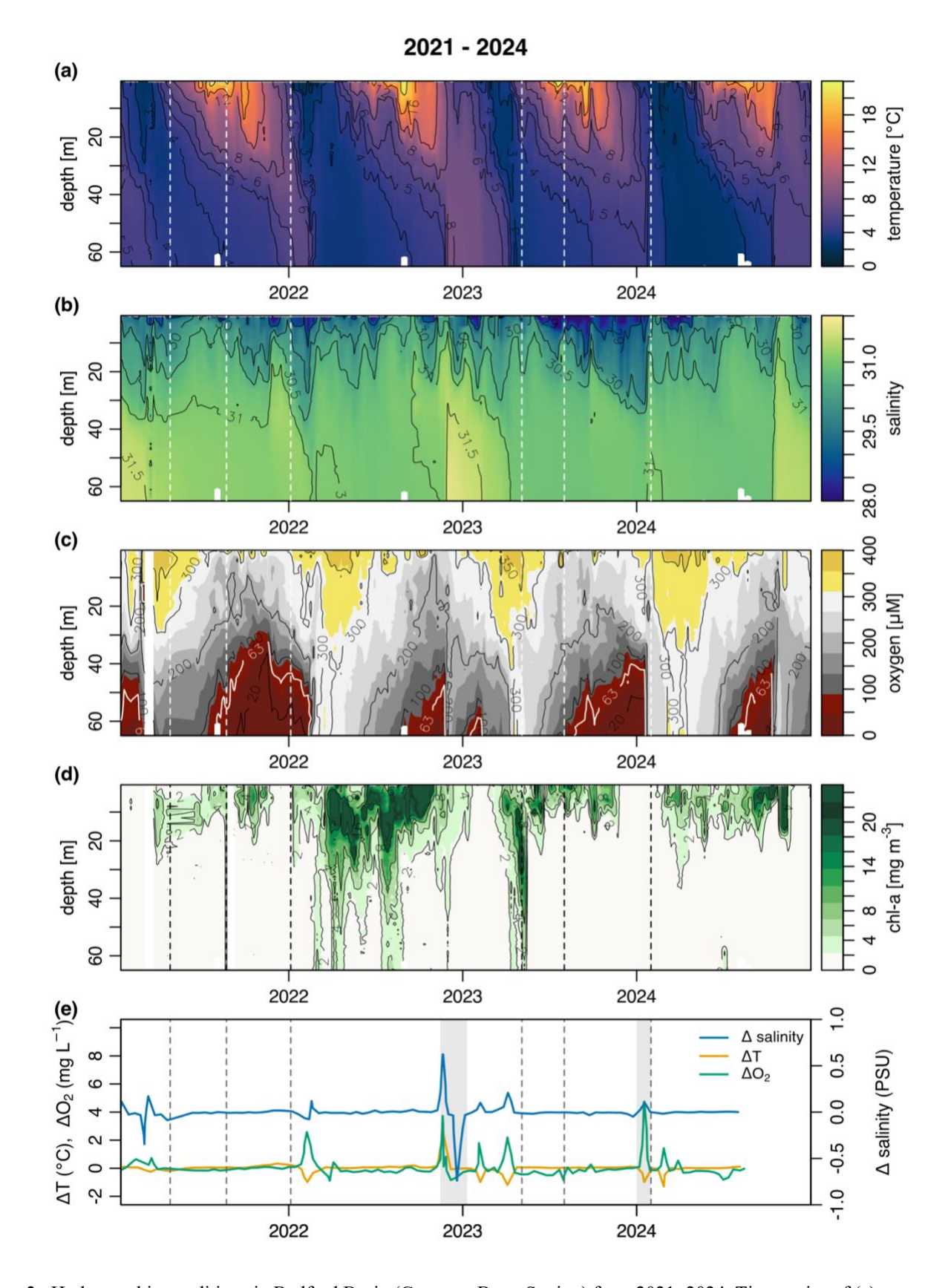


Figure 2: Hydrographic conditions in Bedford Basin (Compass Buoy Station) from 2021–2024. Time series of (a) Temperature (°C), (b) Salinity (PSU), (c) Oxygen concentration (μM), (d) Chl-a concentration (mg m⁻³), (e) anomalies of temperature, oxygen concentration and salinity (T,S,O), which trace the intrusion of shelf waters into the basin. A zero anomaly

represents no variation between T,S,O between weeks. The grey shaded area represents times likely of an intrusion event. Dashed lines in all panels represent the sampling events in this study.

3.2. Total ²³⁴Th in the water column

255

260

265

270

Throughout the water column, 234 Th_{tot} activities displayed large deficits (234 Th_{tot} = 0.1–1.1 dpm L⁻¹) compared to 238 U activities (mean = $^{2.09}$ ± 0.04 dpm L⁻¹) at all sampling events and all depths (Fig. 3). This indicates that the particle flux in Bedford Basin was large enough in the entire water column to scavenge 234 Th prior to its decay. Similar observations have been made in the few other studies from coastal regions (e.g., Luo et al., 2014; Wei and Murray, 1992; Black et al., 2023; Lepore et al., 2007). This contrasts with open ocean sites where 234 Th deficits are typically restricted to the euphotic zone (Owens et al., 2015). Generally, in each season, consistency is seen between years, with some variation that could be due to differences in bloom timing, productivity, etc. The largest deficit, with 234 Th activities as low as 0.1 dpm L⁻¹, occurred during the large bloom event in May 2023 (Fig. 2d), suggesting enhanced scavenging during this time. Winter profiles (Fig. 3c) are more uniform with depth compared to spring and summer, and despite low productivity during these times (Fig. 2d), still show a pronounced deficit throughout the entire water column.

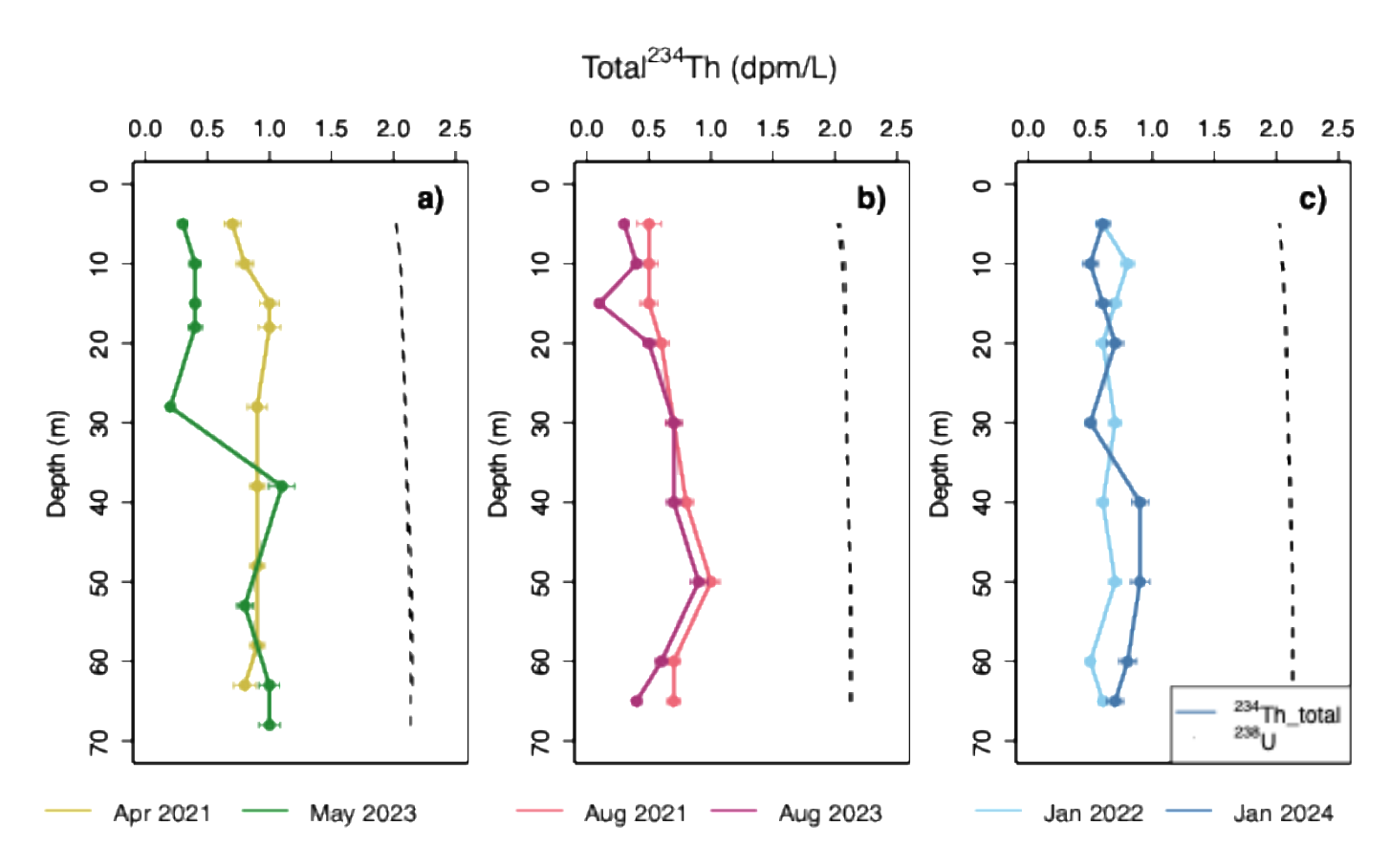
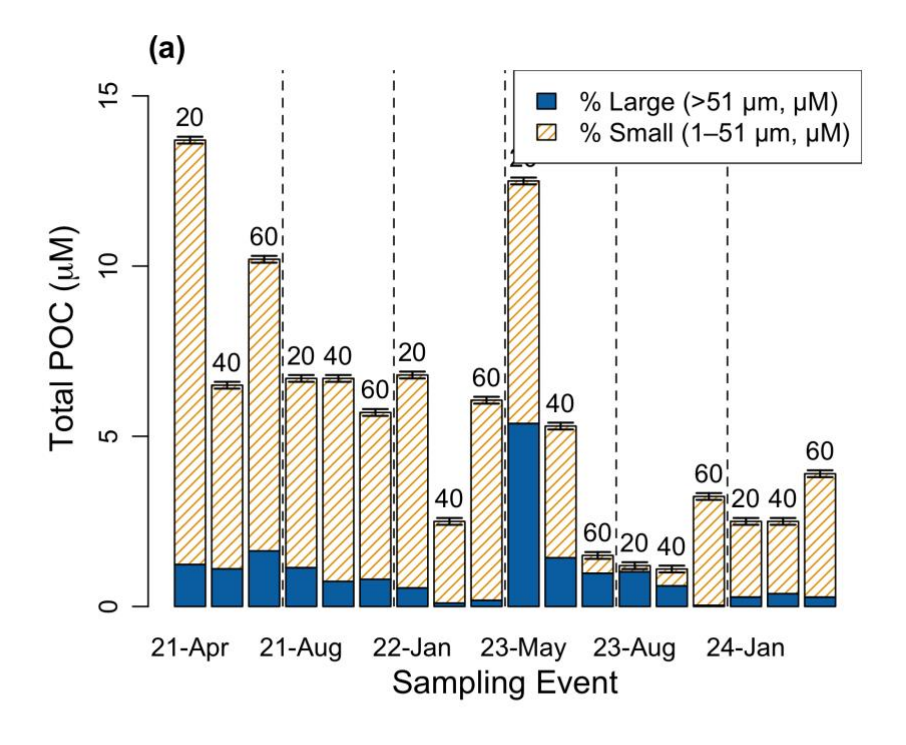


Figure 3: Water column profiles of total 234 Th (dpm L^{-1}) activity in each season sampled. (a) Spring (April, May), (b) Summer (August), (c) Winter (January) compared to 238 U activity (dpm L^{-1}) derived from salinity (Owens et al., 2011).

3.3. Size fractionated particulate ²³⁴Th and POC activities in water column

275 Along with ²³⁴Th_{tot}, size fractionated particulate ²³⁴Th (²³⁴Th_p) were obtained at approximately 20, 40, 60 m depths by in-situ pumps. At all depths, the small (1–51 μm) particle fraction dominated the ²³⁴Th_p activities (93%) and POC concentration (77.4%), suggesting a large amount of POC is suspended on particles in the water column (Fig. 4a). POC on the small particle fraction had a mean of $4.5 \pm 3.1 \,\mu\text{M}$, while POC on the large particle fraction had a mean of $1.0 \pm 1.2 \,\mu\text{M}$. Mean $^{234}\text{Th}_{\text{D}}$ activities on the small size fraction $(0.8 \pm 0.3 \text{ dpm L}^{-1})$ were higher than those on large particles. Mean ²³⁴Th_n activities on large size 280 fraction particles were 0.06 ± 0.04 dpm L^{-1} (Fig. 4b) and were highest during bloom events. This value is significantly larger than first measurements of 234 Th_p in the Bedford Basin (0.008 \pm 0.006 dpm L⁻¹, Black et al., 2023), likely due to a difference in methods (see Section 4.4). Although dissolved ²³⁴Th (²³⁴Th_{diss}) was not measured in this study, subtracting ²³⁴Th_p from the ²³⁴Th_{tot} at the same approximate depth provides an estimation. The activity of dissolved ²³⁴Th in Bedford Basin is consistently low and nearly devoid (0-0.6 dpm L⁻¹), a finding that is similar in other coastal fjords (e.g. Luo et al., 2014). Hence, the majority of ²³⁴Th_{tot} is in the ²³⁴Th_p pool, consistent with other studies in the Bedford Basin (Black et al., 2023; Niven et al., 1995). The 285 residual activity of particulate ²³⁴Th (Rap₂₃₄) reveal that residual beta counts were higher than the detection limit in 38 % of the small particulate samples, but no counts exceeding the detection limit were found on the large particles (Fig. 9).



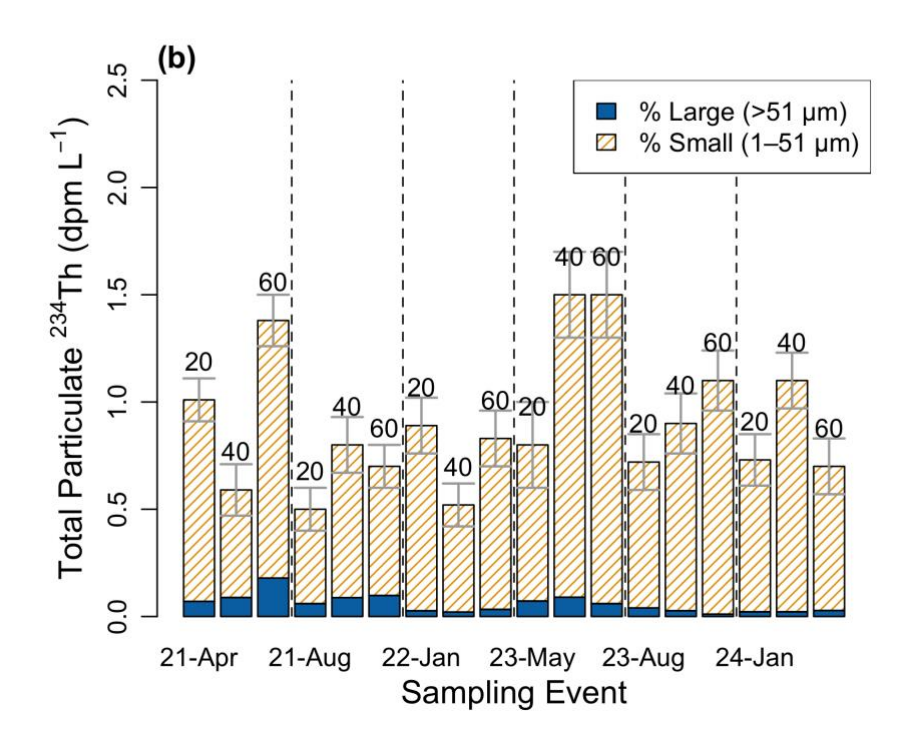


Figure 4: Size-fractionated (1–51 μ m, >51 μ m) pools of (a) particulate organic carbon (μ M) and (b) total particulate ²³⁴Th (dpm L⁻¹) at approximately 20, 40, and 60 m for each sampling event. Bars are stacked and totals equal the sum of the small and large fractions (legend shows % contribution by size class). Numbers above bars indicate approximate sampling depth. Dashed lines separate events. The small fraction generally dominates both POC and ²³⁴Th.

305

310

315

3.4. POC:²³⁴Th ratios on small and large particles

In general, POC: 234 Th on both the large and small particle fractions are < 20 µmol C dpm $^{-1}$ (Fig. 5) and were variable. On average, higher POC: 234 Th ratios on the larger particles were observed compared to the smaller particles (p < 0.01, n=18), consistent with open ocean studies (Charette and Moran, 1999). This trend was most driven by two distinct high ratios on the large fraction in the 0–20 m depth range (May 2023, August 2023), likely driven by a strong chl-a signal at these times (Fig. 2d). The POC: 234 Th ratio on the small and large fraction had a mean of 5.8 ± 4.1 (0.2–13.2) µmol C dpm $^{-1}$ and 16.2 ± 14.3 (range 1.3–67) µmol C dpm $^{-1}$ respectively. The POC: 234 Th ratio generally decreased with depth on the large fraction, but not on the small fraction which showed no pattern with depth (Fig. 5a). On average, the large fraction POC: 234 Th ratios are a factor of ~ 2.8 x larger than the small POC: 234 Th ratios.

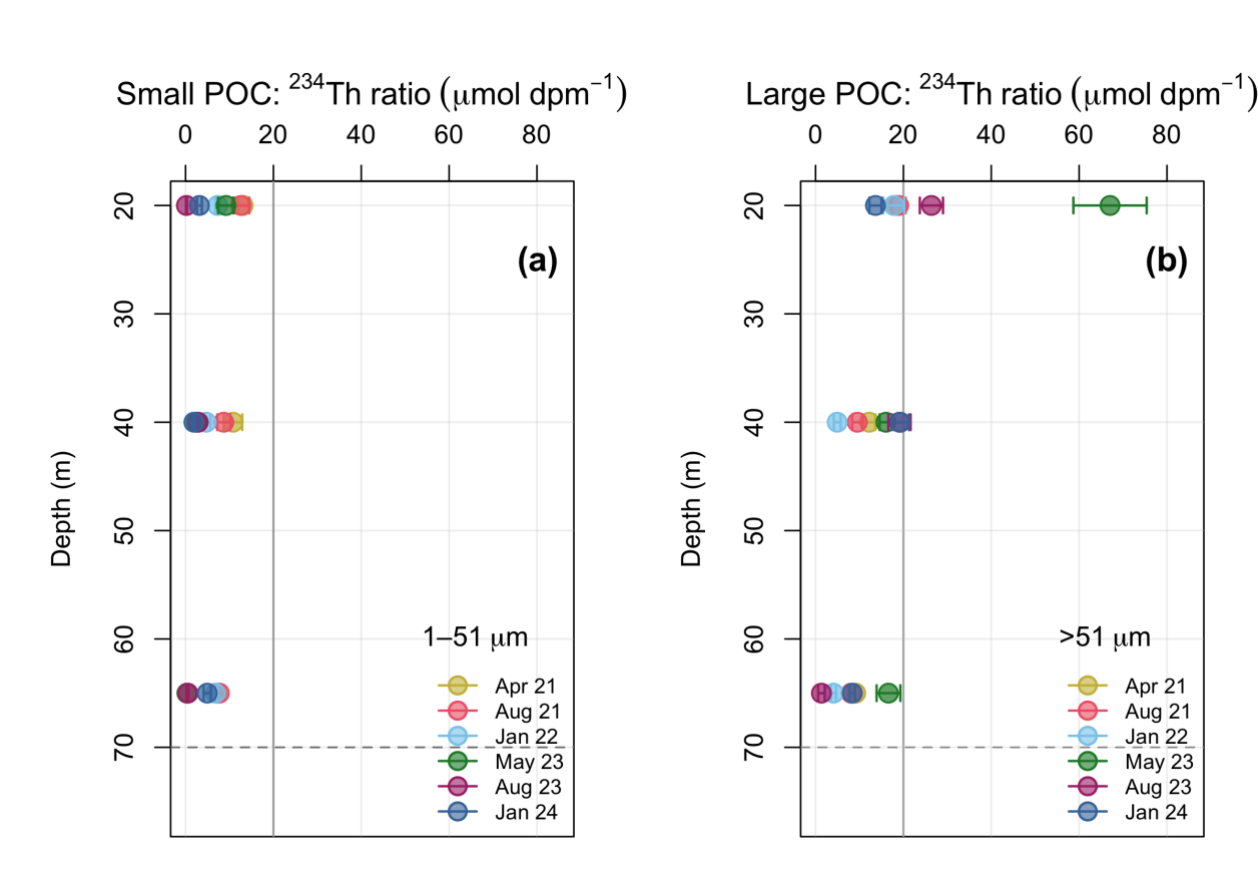


Figure 5: Water column ratios of POC to ²³⁴Th (POC:²³⁴Th; μmol C dpm⁻¹) in each sampling event throughout 2021–2024. Error bars indicate propagated uncertainties associated with measurements. (a) POC:²³⁴Th on the small particle (1–51 μm) fraction (b) POC:²³⁴Th on the large particle (> 51 μm) fraction. Other than a few large POC:²³⁴Th ratios that correspond with greater chl-a in the water column (Fig. 2d), the POC:²³⁴Th ratios are similar in magnitude on both size fractions (< 20 μmol C dpm⁻¹; grey reference line). The dashed grey line at 70 m represents the bottom of the Bedford Basin.

3.5. Water column fluxes of ²³⁴Th and POC

3.5.1. ²³⁴Th fluxes

Cumulative 234 Th fluxes increase nearly linearly with water depth ($R^2 = 0.95$) and do not show much seasonal variation (Fig. 6a). Interestingly, similar observations were made in other coastal sites such as Dabob Bay, Washington (Wei and Murray, 1992),

Saanich Inlet, British Columbia (Luo et al., 2014), Beaufort Sea Shelf (Baskaran et al., 2003), and Mecklenburg Bay, Baltic Sea (Forster et al., 2009). Combining the data from the linear regression of all dates reveals a water column rate increase with depth of 37 dpm m⁻² d⁻¹, larger than previously measured in spring and summer 2019 (31 dpm m⁻² d⁻¹; Black et al., 2023). The mean (\pm s.d.) water column ²³⁴Th fluxes at \sim 65 m and extrapolated to 70 m were 2638 \pm 238 and 2842 \pm 224 dpm m⁻² d⁻¹ respectively.

3.5.2. POC fluxes derived with the small and large particle size fraction

320

325

330

335

POC export fluxes (Fig. 6b, Fig. 6c) were calculated following Eq. 4 using both the small (1–51 μ m) and large (> 51 μ m) POC:²³⁴Th ratios (Fig. 5a and 5b, respectively). Fluxes based on the small size fraction showed no consistent pattern with depth, while fluxes on the large size fraction varied more strongly. Small particle fluxes at 65 m had a mean (\pm s.d.) of 12.5 \pm 7.1 (Fig. 7a) and ranged from 0.8 to 19.6 mmol C m⁻² d⁻¹ (Fig. 6b). In general, large particle fluxes followed a high-low pattern with depth (Martin et al., 1987), and fluxes at 65 m had a mean (\pm s.d.) of 20 \pm 14 mmol C m⁻² d⁻¹ (Fig. 7c) and ranged from 3.6 \pm 1.1 to 44.5 \pm 4.1 mmol C m⁻² d⁻¹. Highest POC flux values were seen in May when chl-a was at its highest (Fig. 6c). Modest POC fluxes were still prevalent in boreal winter estimates, averaging 15.7 \pm 7.2 mmol C m⁻² d⁻¹. One of these winter sampling events occurred around the time of an intrusion event in the Bedford Basin, and it is possible that this event brought additional POC from nearby shelf waters (see Section 4.2). Disregarding this sampling event, POC fluxes in January 2022 were 10.6 \pm 1.5 mmol C m⁻² d⁻¹.

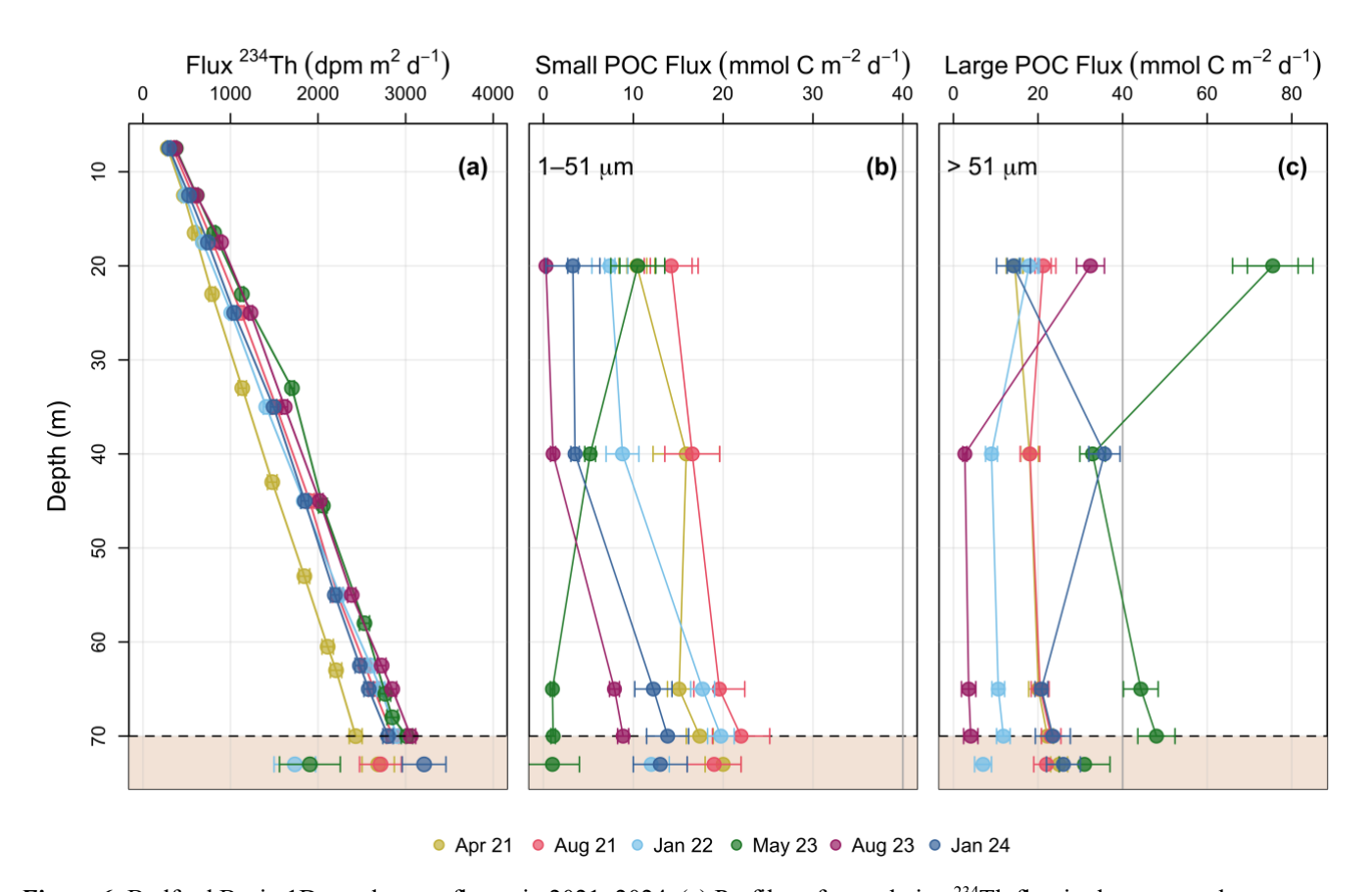


Figure 6: Bedford Basin 1D steady state fluxes in 2021–2024. (a) Profiles of cumulative 234 Th flux in the water column compared to decay corrected excess 234 Th (234 Th_{xs,0}) in the topmost sediment. Sediment inventories of 234 Th_{xs,0} were integrated from \sim 0–EQ depth to derive accumulation of 234 Th_{xs,0} on the sea floor (Eq. 7). The resulting sediment fluxes (i.e. sediment accumulation flux) are shown below the approximate depth of the sediment-water interface (dashed line). POC fluxes on (b) the

small (1–51 μ m) particle fraction, and (c) large (> 51 μ m) particle fraction. The sediment accumulation flux was also multiplied by the water column POC:²³⁴Th ratios (at 60–65 m) to derive POC sediment accumulation flux. Note the change in scale between the plots and the grey reference line at 40 mmol C m⁻² d⁻¹. No sediment core was taken in August 2023.

340

345

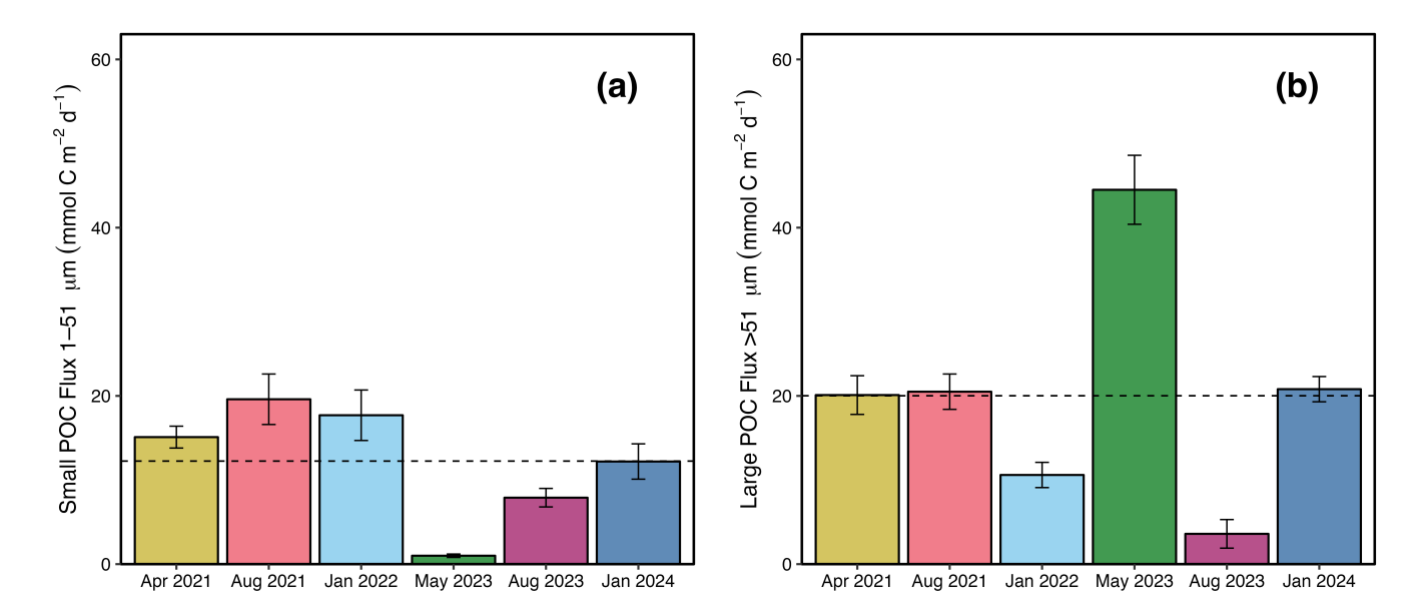


Figure 7: Depositional POC fluxes to the seabed in the Bedford Basin. Measured 234 Th-derived mean (\pm s.d.) particulate organic carbon fluxes deposited to the near bottom (\sim 65 m) of the Bedford Basin on the (a) small particle (1–51 μ m) and (b) large particle (> 51 μ m) size fractions. The dashed black line represents the mean POC flux for each size fraction respectively.

Table 1. Water column ²³⁴Th cumulative fluxes measured at the bottom of the Bedford Basin (60–65 m). Water column ²³⁴Th fluxes are multiplied by the POC:²³⁴Th ratios measured on small and large particles to derive POC fluxes with a steady state model. Note that the sampling events with an asterisk (*) represent data from a pilot study in 2019 (Black et al., 2023).

Sampling	Sampling	Season	Water	Small	Small	Large	Large
Event	Date		Column	particle	particle	particle	particle
			²³⁴ Th flux	POC: ²³⁴ Th	POC flux	POC: ²³⁴ Th	POC flux
	M-D-Y		$dpm \ m^{-2} \ d^{-1}$	μmol C	mmol C m ⁻²	μmol C	mmol C m ⁻²
				dpm^{-1}	d^{-1}	dpm^{-1}	d^{-1}
April 2019*	4-11-2019	Spring	2140 ± 160	11 ± 4	25 ± 10	340 ± 10	780 ± 190
May 2019*	5-09-2019	Spring	1890 ± 150	11 ± 6	20 ± 10	920 ± 4	2070 ± 500
April 2021	04-27-2021	Spring	2205 ± 64	7.1 ± 1	15.1 ± 1.2	9.1 ± 1	20.1 ± 2.3
May 2023	05-05-2023	Spring	2767 ± 62	0.3 ± 0.07	0.8 ± 0.2	67 ± 8.3	44.5 ± 4.1
August 2019*	08-02-2019	Summer	2020 ± 150	60 ± 20	150 ± 40	300 ± 80	710 ± 170
August 2021	08-23-2021	Summer	2537 ± 61	7.7 ± 1	19.6 ± 3.0	8.1 ± 1	20.5 ± 2.1
August 2023	08-02-2023	Summer	2726 ± 50	2.9 ± 0.4	8 ± 0.6	1.3 ± 0.6	3.6 ± 1.7
January 2022	01-05-2022	Winter	2603 ± 46	7.3 ± 1.2	19 ± 3.1	4.1 ± 0.6	10.6 ± 1.5
January 2024	01-31-2024	Winter	2478 ± 54	4.9 ± 0.9	12.2 ± 2.1	8.3 ± 0.7	20.8 ± 1.5

3.5.3. Sediment accumulation fluxes of ²³⁴Th and POC

Excess 234 Th was concentrated in the surface sediments, with the highest activities observed in the top 1.5 cm (Fig. 8a). Excess 234 Th decreased with depth, and equilibrium with supported 234 Th was consistently reached by 4.5–6 cm in every core. Excess 234 Th above the EQ was variable in each sampling event, averaging 15.3 \pm 16 dpm g $^{-1}$ and ranging from 4.8–46 dpm g $^{-1}$ (Fig. 8a). The mean supported 234 Th (from 4.5–6 cm) was 2 \pm 0.5 dpm g $^{-1}$. The mean sedimentary POC concentration was 4.9 \pm 0.4 mmol C g $^{-1}$, with an average (wt %) of 5.7 \pm 0.3 % TOC. POC concentrations were consistent both downcore (0–6 cm) and between cores (n=5), in line with previous studies in the Bedford Basin (Black et al., 2023; Buckley et al., 1995). The POC: 234 Th ratios in sediments were an order of magnitude higher than those in the overlying water column, ranging from 103–3257 µmol dpm $^{-1}$ (Fig. 8b). This difference likely reflects the more rapid decay of 234 Th relative to the remineralization of OC on the seabed. These ratios increased with core depth, corresponding with decreasing 234 Th relative to the remineralization of OC on the seabed. These ratios increased with core depth, corresponding with decreasing 234 Th relative to the remineralization of OC on the seabed. These ratios increased with core depth, corresponding with decreasing 234 Th ratio of water column particles collected at the bottom of the basin (60–65 m) to derive POC sediment accumulation fluxes. The mean (\pm s.d.) POC sediment accumulation flux derived with the small particle fraction was 13 \pm 8 mmol C m $^{-2}$ d $^{-1}$, lower than the mean POC flux derived with the large particle fraction of 22 \pm 9 mmol C m $^{-2}$ d $^{-1}$ (Fig. 6b, Fig. 6c).

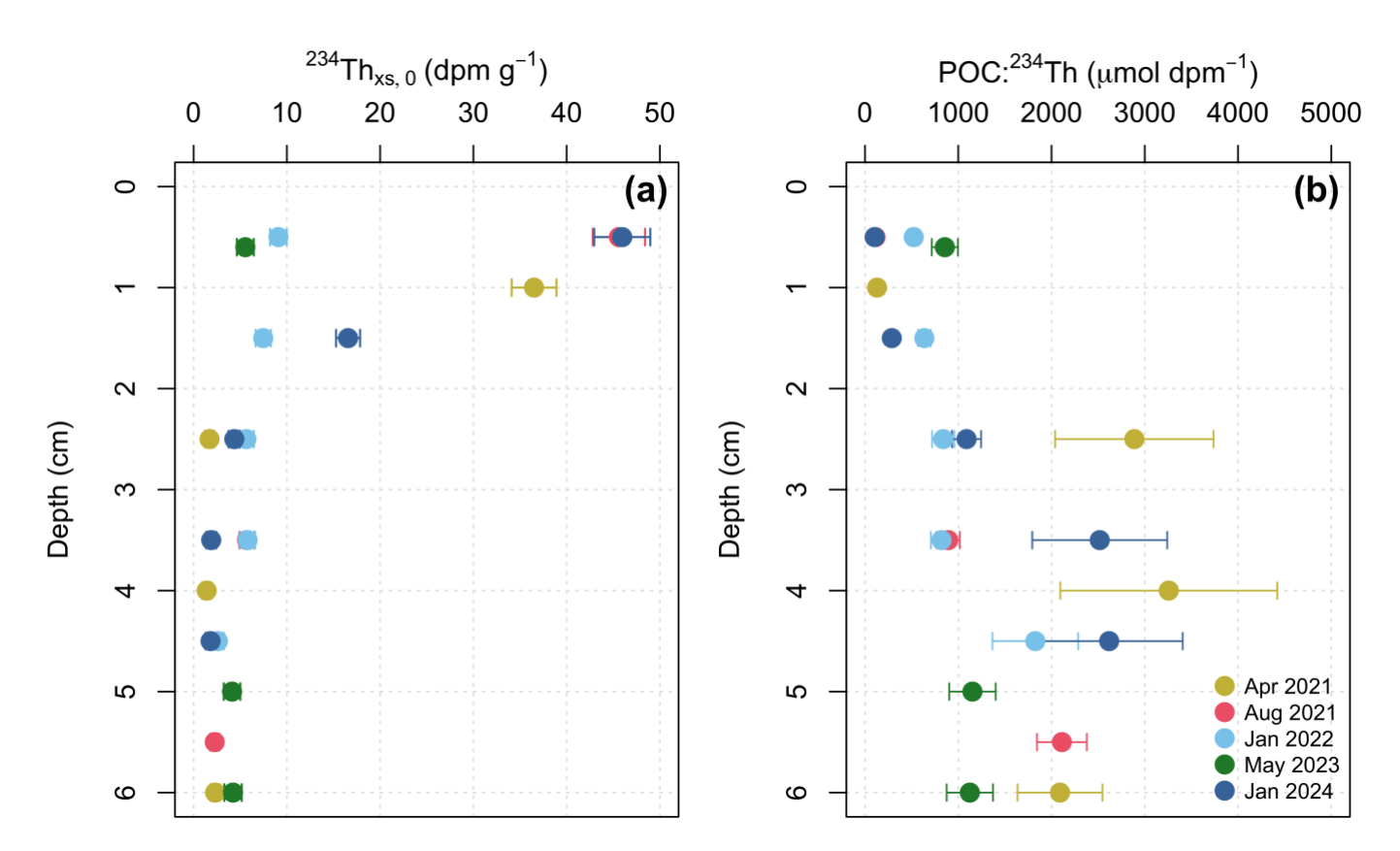


Figure 8: Sediment downcore profile of (a) decay corrected excess 234 Th (234 Th_{xs,0}), derived from subtracting the supported 234 Th from decay corrected 234 Th in sediments. (b) The ratio of POC: 234 Th_{xs,0} in sediments.

Table 2. Bedford Basin sediment accumulation fluxes of ²³⁴Th (dpm m⁻² d⁻¹) in each sampling event in 2021–2024, calculated by multiplying the integrated activities of ²³⁴Th_{xs,0} (0–EQ depth) by dry bulk density and the decay constant for ²³⁴Th. Note that there was no sediment sampling in August 2023.

Sampling Event	Sampling Date (M-D-Y)	Season	²³⁴ Th sediment accumulation flux (dpm m ⁻² d ⁻¹)
April 2021	04-27-2021	Spring	2687 ± 184
May 2023	05-05-2023	Spring	1907 ± 347
August 2021	08-23-2021	Summer	2713 ± 239
January 2022	01-05-2022	Winter	1735 ± 237
January 2024	01-31-2024	Winter	3211 ± 249

4. Discussion

385

390

4.1. A general match between water column ²³⁴Th flux and surficial sediment ²³⁴Th accumulation flux

This study demonstrates the utility of coupled water column-sediment ²³⁴Th measurements in assessing coastal carbon fluxes using a 1D steady-state model. To the best of our knowledge, few studies have applied a coupled water column-sediment approach to explore the ²³⁴Th/²³⁸U method in support of coastal carbon budget quantifications (Cochran et al., 1975; Charette et al., 2001; Lepore et al., 2007; Turnewitsch and Springer, 2001). The present study, along with the first coupled measurements in Bedford Basin made in 2019 (Black et al., 2023), demonstrates a close match between the flux at the bottom of the water column

and the uppermost sediments beneath it. Overall, the mean (\pm s.d.) 2021–2024 sediment accumulation of 234 Th of 2261 \pm 512 matches within error to the mean water column flux (interpolated to 70 m) of 2851 \pm 249 (Fig. 6a). A paired t-test revealed no statistically significant difference between the water column and sediment fluxes, with a mean difference (\pm s.d.) of 349 \pm 747 dpm m⁻² d⁻¹ (t = 1.04; df= 4, p=0.30). When data from 2019 (Black et al., 2023) are included, the mean difference (\pm s.d.) is even smaller (184.1 \pm 836) and not statistically significant (t = 0.6; df=7, p=0.5), suggesting that the observed difference may be due to random variability. The mean ratio between water column and sediment 234 Th fluxes is 1.1 indicating close agreement between the two, with the water column flux being slightly higher than the sediment flux. This finding implies that on the timescales of weeks to ~ 100 days, no major particle loss is occurring, and particles are generally not being exported out of the basin. A similar finding was first made by Cochran et al. (1995) who found a water column-sediment inventory match within a factor of 2 in both 1992 and 1993 on the Northeast Water Polynya off Greenland. Likewise, in their comparison of model predicted 234 Th water column inventory vs sediment inventories in the upper 0–5 cm of the Gulf of Maine, Charette et al. (2001) find that inventories were within a factor of 2 of the predicted values, with a ratio of 1.1. These findings suggest that Bedford Basin is a promising location for more complex observational studies of particle dynamics, and opens the opportunity to study other short-lived radioisotopes, such as Bismuth-210 (210 Bi; $t_{1/2}$ = 5 d) to study particle dynamics on a finer temporal resolution (hours to days; see Yang et al., 2022).

4.2. A persistent year-round deficit of ²³⁴Th in the water column

395

400

405

415

420

425

430

A notable feature of this study is the persistent deficit of ²³⁴Th relative to ²³⁸U in all seasons sampled. Similar findings have been reported in other shallow basins (Luo et al., 2014; Charette et al., 2001; Evangeliou et al., 2011; Amiel and Cochran, 2008). This persistent deficit suggests that i) particle scavenging of ²³⁴Th is occurring throughout the entirety of the water column (0–70 m) and ii) the scavenging rate is high enough to continually maintain a lower ²³⁴Th activity relative to ²³⁸U. Particles in the Bedford Basin may originate from both biological processes in the upper 30 m (Fig. 3), and from resuspension.

Resuspension from the seafloor could be a source of particles to the water column, though multiple lines of evidence indicate it is likely minimal at the Compass Station. First, sedimentary POC:²³⁴Th ratio is an order of magnitude higher than those in the water column (Fig 8b), likely due to the temporal decay of ²³⁴Th exceeding the remineralization of POC. Bottom resuspension would be expected to introduce particles with these elevated POC:²³⁴Th which is not reflected in deep water column POC:²³⁴Th ratios from this study. Second, recent measurements of physical properties in the Bedford Basin report very weak near-bottom currents (typically < 1–2 cm s⁻¹), even during tidal cycles at the Compass Station. Other coastal studies in shallow systems have indicated that near-bed velocities of 20–30 cm s⁻¹ are generally required to erode bottom sediments (Ziervogel et al., 2021). These findings support negligible resuspension from the seafloor at the Compass Station. However, given the concave bathymetric profile of the Bedford Basin (Fig. 1), resuspended sediments could be "funneled" into the Compass Station from the sides (Trimble and Baskaran, 2005). In this study, we observe a strong signal of resuspension at mid depths in April 2021, as well as a weaker signal of resuspension at 60 m in the summer and winter sampling events (Fig. 9), though only on the small particle fraction. This Rap234 signal provides indication that some lateral resuspension of fine particles is likely occurring in the Bedford Basin and is reason to report POC fluxes using the large particle fraction. Furthermore, deep and extensive CTD-derived chl-a fluorescence signals (Fig. 2d) suggest that biological processes could also be responsible for particle creation and continued scavenging in deeper waters. These features are not unique (Black et al., 2023), and fluorescent organic material has been visually observed at depths > 3000 m in the Arctic as a result of a rapid bloom-collapse cycle (Boetius et al., 2013). While additional data (e.g. Underwater Vision Profilers (UVP), net primary production (NPP), backscatter, etc.) are needed to identify the source for the

evident fluorescence signals at depths much deeper than expected given the high particle load (i.e. elevated chl-a and POC: ²³⁴Th) in the water column, these features could be the key to understanding the persistent Th deficits in the Bedford Basin.

435 The persistent deficit is also strong in boreal winter periods, when production is presumed to be at its lowest. As argued by Hargrave and Taguchi (1978), inflows of dense surface water from intrusions could deliver additional organic material that could drive the moderate POC fluxes we see at this time. Therefore, the POC flux in January 2024 could be attributed to the intrusion event occurring around the same time. However, our sampling in January 2022 still yields a modest flux value of 10.6 ± 1.5 mmol C m⁻² d⁻¹ at 65 m. This is comparable to January 2024 (Fig. 7) but took place after a period of water column stability (Fig. 440 2e). A notable feature of this 2022 winter event is that POC fluxes are higher when using the small fraction to compute flux, yielding 17.7 ± 1.3 mmol C m⁻² d⁻¹ (Fig. 7a). Small phytoplankton ($< 20 \mu m$) can play an important role in carbon export and biogeochemical cycling and have been shown to contribute substantially to biomass in the North Atlantic, with some species especially dominant in subpolar regions during winter months (Bolaños et al., 2020). Robicheau et al. (2022) have shown that specific phytoplankton types have higher abundance values, especially in the early winter in the Bedford Basin when there are 445 temperature anomalies. Primary production was not measured in this study, but modelling efforts have shown that the NPP in the Bedford Basin is in the 100's of mmol C m⁻² d⁻¹ at peak times, and 10's of mmol C m⁻² d⁻¹ otherwise (Black et al., 2023), suggesting that lower NPP in winter months can still yield modest POC fluxes. This was also observed in the nearby Gulf of Maine (Charette et al., 2001) where POC fluxes of 14 ± 0.8 mmol C m⁻² d⁻¹ were measured in the lower range of their NPP measurements (26.4 mmol C m⁻² d⁻¹). These small cells could possibly be the driver of this distinct winter flux (most prominent 450 in the small particle fraction) that we see in January 2022, though the reasoning behind the winter flux remains ambiguous. These results highlight the dynamic particle processes in Bedford Basin that maintain persistent ²³⁴Th deficits, emphasizing the need for continued year-round, high-resolution particle and radionuclide measurements.

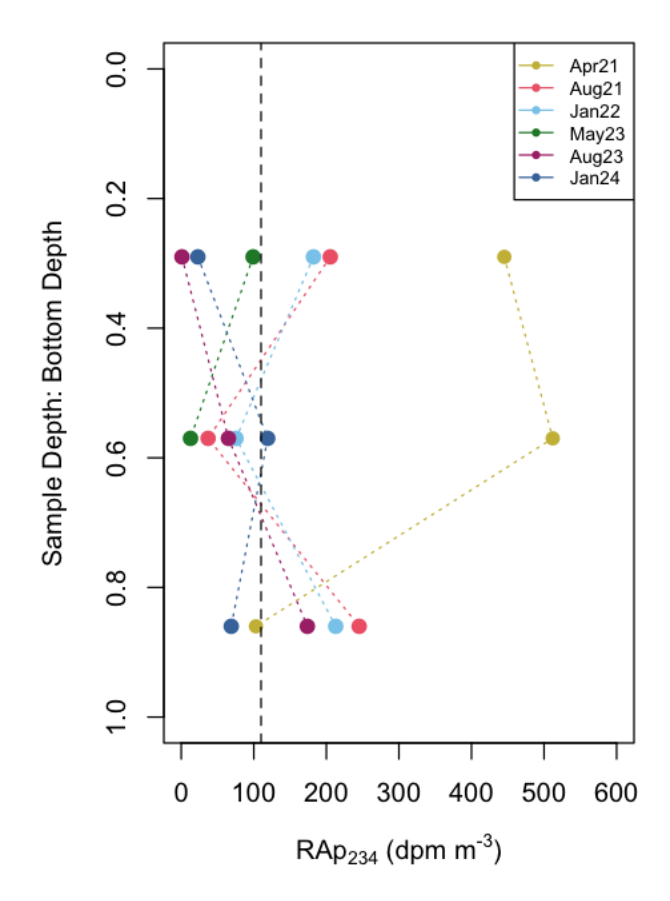


Figure 9: Profiles of the total residual activity of particulate 234 Th (Ra_{P234}) at the Compass Station vs normalized depth calculated as sample depth divided by total water depth (0 = surface, 1 = bottom). Ra_{P234} values represent the sum of residual counts from both size fractions. Only Ra_{P234} signals above the detection limit were found on the small particulate fraction. The dashed vertical line is the detection limit (derived from filter blank analyses).

4.3. Non-steady state (NSS) & lateral heterogeneity considerations

455

460

465

470

Steady-state (SS) dynamics are often assumed in coastal and open ocean ²³⁴Th/²³⁸U disequilibrium studies (e.g. Coale and Bruland, 1985; Foster and Shimmield, 2002) due to sampling constraints. Fluxes in coastal zones can however be impacted by lateral advection and non-steady state conditions, though the absolute value of each of these impacts on the total flux of ²³⁴Th is difficult to evaluate without greater spatial and temporal resolution of ²³⁴Th sampling. Thus, the SS model is applied here, and we explore the implications of NSS factors in this section.

In this study, we assume that ∂^{234} Th/ ∂ t is equal to 0 and the system is in steady state. The SS model assumes that i) 234 Th activities and removal rates are near constant with respect to 234 Th decay, ii) the contributions of vertical and horizontal advection of 234 Th are minor, and iii) scavenging is irreversible. Physical studies of the Bedford Basin have generally shown that 1D assumptions hold for most of the year (Burt et al., 2013), and modelling efforts have demonstrated that \sim 80 % of particles that originate in the basin stay in the basin (Shan and Sheng, 2012). The circulation pattern of Halifax Harbour is characterized as a two-layer, estuarine-type system, with a fresher upper layer flowing seaward, driven by inflows from the Sackville River,

and a saltier deep-water return flow (Fader and Miller, 2008). However, with a mean surface outflow of $0.2~\rm cm~s^{-1}$, this circulation is weakest in the Bedford Basin (Burt et al., 2013). Despite an inflow from the open Atlantic, the presence of a sill largely prevents mixing below 20 m in the basin (Shan et al., 2011). Although our observations come from a single, centrally located station, we acknowledge that lateral heterogeneity and edge effects may influence 234 Th and POC dynamics in the Bedford Basin, especially from $0-20~\rm m$. To assess this, we evaluated a surface lateral 234 Th contribution using our $0-20~\rm m$ mean 234 Th activity, a 3 km cross-basin scale, and observed basin current velocities ($0.2~\rm cm~s^{-1}$). For a theoretical 50 % cross basin difference in 234 Th activities, the lateral 234 Th flux contribution is $\sim 346~\rm dpm~m^{-2}~d^{-1}$, which is $\sim 52~\rm \%$ of our mean surface cumulative flux, and $\sim 14~\rm \%$ of the full water column flux to 65 m. This suggests that even under a strong 50 % contrast, the full water column budget changes only modestly. These lateral 234 Th flux estimates are intended as a first order, illustrative calculation, and real cross-basin gradients 234 Th activities (if any) should be measured for a more robust estimate of lateral contributions in future studies.

NSS impacts (rapid temporal changes in ²³⁴Th activities) have been shown to play a role on flux estimates during phytoplankton blooms, and prior studies have shown that NSS terms during blooms can alter ²³⁴Th export fluxes often by 10–50% (Buesseler et al., 1992; Ceballos-Romero et al., 2018). To assess how these departures from SS may impact our reported fluxes, we applied theoretical NSS sensitivities to our spring profiles. Assuming a modest NSS term (0.003 dpm L⁻¹ d⁻¹), the NSS correction is 7.8% of our reported SS ²³⁴Th flux. Under an upper bound scenario with a larger NSS term (0.01 dpm L⁻¹ d⁻¹), the resulting NSS correction increases to ~ 25.8 % of the spring SS estimate. These theoretical corrections show that though minor, NSS effects can become significant during rapid bloom events. Periodic deep vertical mixing, such as during an intrusion event could increase the potential to disrupt the validity of the SS model. Indeed, we do see some indication of mixing multiple times throughout the study period (Fig. 2e), however, no major lines of evidence in the ²³⁴Th activities are indicated in our study (no major Ra_{P234} signals, or significant difference in POC:²³⁴Th), and despite intrusion events, the ²³⁴Th_{tot} activities are similar between January 2024 (intrusion) and January 2022 (no intrusion). These observations may suggest that the Bedford Basin rapidly re-establishes a ²³⁴Th deficit following intrusion or mixing events and implies that particle scavenging and export are strong and continuous. If

feasible, future studies in the basin should sample on a finer temporal resolution (1-4 weeks) to better understand NSS

4.4. Revisiting 234 Th activities on $> 51 \mu m$ particles

contributions in the basin.

475

480

485

490

495

500

505

510

A key source of uncertainty in estimating POC fluxes using ²³⁴Th/²³⁸U disequilibrium is the POC:²³⁴Th ratio used for filtered particles, which has led to inconsistent flux estimates in previous studies (Lalande et al., 2008). Determining the most representative POC:²³⁴Th ratio remains an active area of research (e.g. Buesseler et al., 2006; Puigcorbe et al., 2020) to ensure accurate flux measurements. In the Bedford Basin, we find the primary source of variability in POC flux estimates is the POC:²³⁴Th ratio of large (> 51 μm) particles. Previously, Black et al. (2023) reported ratios in the Bedford Basin > 900 μmol dpm⁻¹, yielding exceptionally large fluxes (~ 2100 mmol C m⁻² d⁻¹, Table 2), over an order of magnitude greater than predicted coastal carbon export models (Siegel et al., 2014). By contrast, this present study finds lower, more modest fluxes (< 70 mmol C m⁻² d⁻¹), consistent with other coastal studies (< 200 mmol C m⁻² d⁻¹, Luo et al., 2014; Cai et al., 2015; Cochran et al., 1995). High POC:²³⁴Th ratios (> 100 μmol dpm⁻¹) have been previously linked to seasonal variability (Charette et al., 2001), however, the extreme values in Black et al. (2023) likely result from the differences in particle collection and delayed counting of beta emissions. Variations in sampling approaches highlight the potential for significant differences in POC measurements. Black et al. (2023) used a vacuum filtration system on Niskin-bottle collected samples, while this study employed McLaneTM Large

Volume Pumps that filter in-situ. In their comparative study (Graff et al., 2023) found that in-situ pump sampling resulted in substantially different POC concentrations compared to Niskin sampling at similar depths. This difference may arise due to variability in filtration speed, particle solubilization (Buesseler et al., 1995), and size fractionation (Hung et al., 2012). The methodological differences suggest that the elevated large particle POC:²³⁴Th ratios reported by Black et al. (2023) likely result from sampling artifacts rather than true variability in particle flux. The ratios obtained in this study provide a more representative measure of large particle POC:²³⁴Th at this site. To improve comparability, future studies in the Bedford Basin and other coastal regions should adopt consistent sampling methods to minimize methodological biases.

4.5. POC export in the Bedford Basin and an estimated C budget

515

520

525

530

535

540

545

550

The POC export fluxes derived in this study are in good agreement with other estimates of carbon fluxes taken in the Bedford Basin (Table 3). The mean depositional organic carbon flux (at 65 m), derived here from the large particle POC: 234 Th ratio and integrated 234 Th flux was 20 ± 14 mmol C m⁻² d⁻¹ (Fig. 7), two orders of magnitude lower than first estimates of 234 Th derived POC flux (Black et al., 2023). This is a similar range as the nearby Gulf of Maine (34 ± 44 mmol C m⁻² d⁻¹; March, June, September; Charette et al., 2001), Saanich Inlet in western Canada ($^{11.5}$ ± 4 mmol C m⁻² d⁻¹; Luo et al., 2014), Greenland continental shelf (25 ± 14 mmol C m⁻² d⁻¹; Cochran et al., 1995), and Norwegian fjords ($^{21.9}$ -24.4 mmol C m⁻² d⁻¹; Wassmann, 1984). Our measured values are also similar to model estimates of organic carbon deposition flux in the Bedford Basin ($^{25.2}$ mmol C m⁻² d⁻¹; Rakshit et al., 2025), and sediment trap estimates at 60 m (17 mmol C m⁻² d⁻¹; Hargrave and Taguchi., 1976). Translated to an annual molar estimate, (assuming our spring, summer, winter mean is representative of the year, and multiplying the mean daily flux by 365), our study reveals that $^{7.3}$ ± 5.1 mol C m⁻² yr⁻¹ is delivered to the seafloor annually, similar to annual mean trap estimates in the Bedford Basin of 6.2 mol C m⁻² yr⁻¹ (Hargrave and Taguchi, 1976). The modeled daily benthic carbon flux in the Bedford Basin of 19 mmol C m⁻² d⁻¹ (Black et al., 2023), is equivalent to an annual export of $^{\sim}$ 7 mol C m⁻² yr⁻¹, also consistent with our 234 Th-based estimates.

Using the mean wt % POC in the upper 5 cm of the sediment cores (5.7 %), mean sedimentation rate (0.2 cm yr⁻¹; Black et al., 2023) and mean dry bulk density (275 kg m⁻³), we find an organic carbon burial rate of 6.9 mmol C m⁻² d⁻¹. This burial rate, combined with our mean POC depositional flux at 65 m, implies that the carbon burial efficiency is ~33%, larger than previous estimates at this site (10 %; Black et al., 2023), and similar to other coastal zones (Faust and Knies., 2019). The remaining ~ 67 % of the depositional POC is remineralized before burial, a finding consistent with measured dissolved inorganic carbon (DIC) fluxes from the sediments (15.6 mmol DIC m⁻² d⁻¹; Rakshit et al., 2025). These findings suggest that the Bedford Basin is an important site of organic carbon sequestration. To better understand C dynamics in the ocean, carbon flux metrics have been developed that help define the efficiency of the Biological Carbon Pump in marine environments (Buesseler et al., 2020; Buesseler and Boyd 2009). The thorium export efficiency ratio (ThE-ratio) is the ratio of POC flux (based on ²³⁴Th measurements) relative to NPP in the euphotic zone. To estimate the ThE-ratio in the Bedford Basin, we divide the annual mean flux of POC measured in this study by the annual mean primary production in the basin. Primary production is rarely measured directly in the Bedford Basin with only one record of NPP from incubation studies (50 mmol C m⁻² d⁻¹; Platt, 1975). Black et al. (2023) approximated an annual mean NPP of 66 mmol C m⁻² d⁻¹ (range 0.4-184 mmol C m⁻² d⁻¹) using a model based on in-situ chl-a and PAR data, which falls within regional estimates from the nearby Gulf of Maine (26–399 mmol C m⁻² d⁻¹; Charette et al., 2001). Using this NPP and our mean POC export at the base of the euphotic zone (~ 20 m; 29.4 mmol C m⁻² d⁻¹), the export efficiency (ThE) is 44.5 %. Applying a \pm 20 % sensitivity to NPP shifts ThE to \sim 37–56 %. This ThE ratio is comparable to other coastal sites (26%, Charette et al., 2001; 50%, Falkowski et al., 1988; 60%, Cochran et al., 1995). A ThE ratio of 44.5 %

suggests moderate export efficiency at our site. It is, however, important to note that our estimation relies on modeled NPP values and updated in-situ measurements of NPP would yield a more precise value of these ThE estimates.

Table 3. An updated carbon budget of the Bedford Basin. Carbon fluxes derived in this study alongside comparable carbon flux measurements in the Bedford Basin. The measured fluxes reported in Black et al. (2023), which likely arise from their different particle sampling approach, are excluded here to enable a meaningful comparison.

Carbon fluxes in the Bedford Basin			
Fluxes in the water column	mmol C m ⁻² d ⁻¹	Methodology	
Large particle POC flux (60–65 m)	20 ± 14	POC: ²³⁴ Th	
Small particle POC flux (60–65 m)	12 ± 7	POC: ²³⁴ Th	
Total particulate flux ^a (60 m)	17	Cylindrical traps	
Modelled POC flux ^b	25.2	Reaction-transport model	
Modelled POC flux ^c	19	Chl-a model	
Fluxes in the sediment	mmol C m ⁻² d ⁻¹	Methodology	
Large particle sediment accumulation flux	22 ± 9	POC: ²³⁴ Th	
Small particle sediment accumulation flux	13 ± 8	POC: ²³⁴ Th	
Measured DIC flux ^b	15.6 ± 10	Pore-water extraction	

^a Total particulate carbon flux from cylindrical trap estimates (Hargrave and Taguchi, 1978). Sediment traps did not have an efficiency correction and may not be limited to POC.

555

560

565

570

575

580

5. Conclusions

This study demonstrates the utility of the coupled 234 Th water column–surficial sediment sampling approach by quantifying 234 Th and POC fluxes in the water column and surface sediments of Bedford Basin, a coastal fjord in the North Atlantic, over quasiseasonal sampling campaigns from 2021 to 2024. Within the uncertainties of the 234 Th/ 238 U disequilibrium method and a steady state approach, we find that the integrated deficit of 234 Th in the water column matches the excess of 234 Th in the uppermost sediments well. The match suggests that, on a timescale of the ~ 100 days, the Bedford Basin is in balance with respect to 234 Th, and no major particle loss is occurring. There were significant deficits of 234 Th relative to its parent 238 U throughout the water column during all sampling events, including boreal winter. We conclude that the majority of 234 Th_{tot} in the Bedford Basin is associated with the particulate 234 Th pool, with a significant portion bound to the small (1–51 μ m) particle fraction. Translated into POC fluxes, the observed deficits reveal a mean POC export flux to the seafloor of 20 ± 14 mmol C m⁻² d⁻¹. This estimate is based on the integrated 234 Th flux between (0–65 m water depth) multiplied by the POC: 234 Th ratio on large (> 51 μ m) particles and is on par with other carbon flux proxies in the area. Water column POC flux estimates showed no apparent trend with season, other than a slightly elevated flux corresponding to elevated chl-a in May 2023. Measurements of POC export in boreal winter reveal modest flux, despite lower chl-a signals at this time. We estimate a thorium export ratio of 44.5 % and an organic carbon burial efficiency of 33 %, higher than previously estimated at this site. Based on this data, we

^b From Rakshit et al. (2025).

^c Model derived from Black et al. (2023) using chl-a measurements.

suggest that the biological carbon pump is moderately efficient in the Bedford Basin, and that this site, like many other coastal areas, is an important site of organic carbon sequestration.

Data Availability: Data to be uploaded to https://www.bco-dmo.org/

Author Contributions: MH: Conceptualization, Formal Analysis, Investigation, Methodology, Visualization, Writing – original draft, Writing – review & editing. EB: Conceptualization, Investigation, Writing – review & editing. CA: Conceptualization, Investigation, Methodology, Resources, Writing – review & editing. MA: Formal Analysis, Methodology, Writing – review & editing. SK: Conceptualization, Funding acquisition, Investigation, Supervision, Writing – Review & Editing. Competing Interests The contact author has declared that none of the authors have any competing interests.

Acknowledgements: This research was supported by the Ocean Frontier Institute (OFI), Natural Sciences and Engineering Research Council of Canada (NSERC), Nova Scotia Graduate Scholarship (NSGS). The authors would like to thank the crew of the Connor's Diving Ltd. vessel EASTCOM, Laura deGelleke, Richard Cheel, Subhadeep Rakshit, and Adam White for assistance in the field. We thank the Bedford Institute of Oceanography for maintaining the time series station at the Bedford Basin and making the data accessible. We thank Claire Normandeau (Dalhousie CERC.OCEAN) and Joshua Landis (Dartmouth College) for analytical assistance.

References:

590

- Aller, R. C., & Cochran, J. K. (1976). 234Th/238U disequilibrium in near-shore sediment: Particle reworking and diagenetic time scales. *Earth and Planetary Science Letters*, 29(1), 37–50. https://doi.org/10.1016/0012-821X(76)90024-8
- Amiel, D., & Cochran, J. K. (2008). Terrestrial and marine POC fluxes derived from 234Th distributions and δ13C measurements on the Mackenzie Shelf. *Journal of Geophysical Research: Oceans*, 113(C3), C03S13.
 https://doi.org/10.1029/2007JC004260
 - Baskaran, M., Swarzenski, P. W., & Porcelli, D. (2003). Role of colloidal material in the removal of 234Th in the Canada Basin of the Arctic Ocean. *Deep-Sea Research Part I: Oceanographic Research Papers*, 50(10–11), 1353–1373. https://doi.org/10.1016/S0967-0637(03)00140-7
- Bhat, S. G., Krishnaswami, S., Lal, D., Rama, & Moore, W. S. (1969). 234Th/238U ratios in the oceans. *Earth and Planetary Science Letters*, 5, 483–491.
 - Black, E. E., Algar, C. K., Armstrong, M., & Kienast, S. S. (2023). Insights into constraining coastal carbon export from radioisotopes. *Frontiers in Marine Science*, 10, 1254316. https://doi.org/10.3389/fmars.2023.1254316
 - Boetius, A., Albrecht, S., Bakker, K., ... Wenzhöfer, F., & RV Polarstern ARK27-3 Shipboard Science Party. (2013). Export of algal biomass from the melting Arctic sea ice. *Science*, 339(6126), 1430–1432. https://doi.org/10.1126/science.1231346
- Bolaños, L. M., Karp-Boss, L., Choi, C. J., ... Giovannoni, S. J. (2020). Small phytoplankton dominate western North Atlantic biomass. *The ISME Journal*, 14(7), 1663–1674. https://doi.org/10.1038/s41396-020-0636-0
 - Buckley, D. E., Smith, J. N., & Winters, G. V. (1995). Accumulation of contaminant metals in marine sediments of Halifax Harbour, Nova Scotia: Environmental factors and historical trends. *Applied Geochemistry*, 10(2), 175–195. https://doi.org/10.1016/0883-2927(94)00053-9

- Buesseler, K. O., Andrews, J. A., Hartman, M. C., Belastock, R., & Chai, F. (1995). Regional estimates of the export flux of particulate organic carbon derived from thorium-234 during the JGOFS EqPac program. *Deep-Sea Research Part II: Topical Studies in Oceanography*, 42(2–3), 777–804. https://doi.org/10.1016/0967-0645(95)00043-P
 - Buesseler, K. O., Antia, A. N., Chen, M., ... Trull, T. (2007). An assessment of the use of sediment traps for estimating upper-ocean particle fluxes. *Journal of Marine Research*, 65(3), 345–416. https://doi.org/10.1357/002224007781567621
- Buesseler, K. O., Bacon, M. P., Cochran, J. K., & Livingston, H. D. (1992). Carbon and nitrogen export during the JGOFS North Atlantic Bloom Experiment estimated from 234Th:238U disequilibria. *Deep-Sea Research*, 39(7–8), 1115–1137.
 - Buesseler, K. O., Benitez-Nelson, C. R., Moran, S. B., ... Wilson, S. (2006). An assessment of particulate organic carbon to thorium-234 ratios in the ocean and their impact on the application of 234Th as a POC flux proxy. *Marine Chemistry*, 100(3–4), 213–233. https://doi.org/10.1016/j.marchem.2005.10.013
- Buesseler, K. O., & Boyd, P. W. (2009). Shedding light on processes that control particle export and flux attenuation in the twilight zone of the open ocean. *Limnology and Oceanography*, 54(4), 1210–1232. https://doi.org/10.4319/lo.2009.54.4.1210
 - Buesseler, K. O., Boyd, P. W., Black, E. E., & Siegel, D. A. (2020). Metrics that matter for assessing the ocean biological carbon pump. *Proceedings of the National Academy of Sciences*, 117(18), 9679–9687. https://doi.org/10.1073/pnas.1918114117
- Buesseler, K. O., Lamborg, C. H., Boyd, P. W., ... Wilson, S. (2007). Revisiting carbon flux through the ocean's twilight zone. *Science*, 316(5824), 567–570. https://doi.org/10.1126/science.1137959
 - Burt, W. J., Thomas, H., Fennel, K., & Horne, E. (2013). Sediment–water column fluxes of carbon, oxygen and nutrients in Bedford Basin, Nova Scotia, inferred from 224Ra measurements. *Biogeosciences*, 10(1), 53–66. https://doi.org/10.5194/bg-10-53-2013
- Burt, W., Rackley, S., Izett, R., ... Cross, T. (2024). Planetary Technologies' groundbreaking marine carbon dioxide removal (mCDR) project in Halifax, and the emergence of Halifax as a global mCDR hub. *OCEANS* 2024 Halifax, 1–6. https://doi.org/10.1109/OCEANS55160.2024.10754096
 - Butman, C. A. (1989). Sediment-trap experiments on the importance of hydrodynamical processes in distributing settling invertebrate larvae in near-bottom waters. *Journal of Experimental Marine Biology and Ecology*, 134(1), 37–88. https://doi.org/10.1016/0022-0981(90)90055-H
- Cai, P., Dai, M., Lv, D., & Chen, W. (2006). An improvement in the small-volume technique for determining thorium-234 in seawater. *Marine Chemistry*, 100(3–4), 282–288. https://doi.org/10.1016/j.marchem.2005.10.016
 - Cai, Y., Guo, L., Wang, X., & Aiken, G. R. (2015). Abundance, stable isotopic composition, and export fluxes of DOC, POC, and DIC from the Lower Mississippi River during 2006–2008. Journal of Geophysical Research: Biogeosciences, 120(11), 2273–2288. https://doi.org/10.1002/2015JG003139.
- 650 Ceballos-Romero, E., Buesseler, K. O., & Villa-Alfageme, M. (2022). Revisiting five decades of 234Th data: A comprehensive global oceanic compilation. *Earth System Science Data*, 14(6), 2639–2679. https://doi.org/10.5194/essd-14-2639-2022
 - Ceballos-Romero, E., De Soto, F., Le Moigne, F. A. C., García-Tenorio, R., & Villa-Alfageme, M. (2018). 234Th-derived particle fluxes and seasonal variability: When is the SS assumption reliable? Insights from a novel approach for carbon flux simulation. *Geophysical Research Letters*, 45(24). https://doi.org/10.1029/2018GL079968
- Charette, M. A., & Moran, S. B. (1999). Rates of particle scavenging and particulate organic carbon export estimated using 234Th as a tracer in the subtropical and equatorial Atlantic Ocean. *Deep-Sea Research Part II: Topical Studies in Oceanography*, 46(5), 885–906. https://doi.org/10.1016/S0967-0645(99)00006-5
 - Charette, M. A., Moran, S. B., Pike, S. M., & Smith, J. N. (2001). Investigating the carbon cycle in the Gulf of Maine using the natural tracer thorium-234. *Journal of Geophysical Research: Oceans*, 106(C6), 11553–11579.
- 660 https://doi.org/10.1029/1999JC000277

- Clevenger, S. J., Benitez-Nelson, C. R., Drysdale, J., Pike, S., Puigcorbé, V., & Buesseler, K. O. (2021). Review of the analysis of 234Th in small-volume (2–4 L) seawater samples: Improvements and recommendations. *Journal of Radioanalytical and Nuclear Chemistry*, 329(1), 1–13. https://doi.org/10.1007/s10967-021-07772-2
- Coale, K. H., & Bruland, K. W. (1985). 234Th:238U disequilibria within the California Current. *Limnology and Oceanography*, 30(1), 22–33. https://doi.org/10.4319/lo.1985.30.1.0022
 - Cochran, J. K., Barnes, C., Achman, D., & Hirschberg, D. J. (1995). Thorium-234/uranium-238 disequilibrium as an indicator of scavenging rates and particulate organic carbon fluxes in the Northeast Water Polynya, Greenland. *Journal of Geophysical Research: Oceans*, 100(C3), 4399–4410. https://doi.org/10.1029/94JC01954
- Environment and Climate Change Canada. (2018). Historical climate data: Halifax International Airport [Dataset]. https://climate.weather.gc.ca/historical data/...
 - Evangeliou, N., Florou, H., & Scoullos, M. (2011). POC and particulate 234Th export fluxes estimated using 234Th/238U disequilibrium in an enclosed eastern Mediterranean region (Saronikos Gulf and Elefsis Bay, Greece) on seasonal scale. *Geochimica et Cosmochimica Acta*, 75(19), 5367–5388. https://doi.org/10.1016/j.gca.2011.04.005
- Fader, G. B. J., & Miller, R. O. (2008). *Surficial geology, Halifax Harbour, Nova Scotia* (p. 590). Natural Resources Canada. https://doi.org/10.4095/224797
 - Falkowski, P. G., Flagg, C. N., Rowe, G. T., Smith, S. L., Whitledge, T. E., & Wirick, C. D. (1988). The fate of a spring phytoplankton bloom: Export or oxidation? *Continental Shelf Research*, 8(5–7), 457–484. https://doi.org/10.1016/0278-4343(88)90064-7
- Faust, J. C., & Knies, J. (2019). Organic matter sources in North Atlantic fjord sediments. *Geochemistry, Geophysics, Geosystems*, 20(6), 2872–2885. https://doi.org/10.1029/2019GC008382
 - Fennel, K., Long, M. C., Algar, C., ... Whitt, D. B. (2023). Modeling considerations for research on ocean alkalinity enhancement (OAE). *EGUsphere*. https://doi.org/10.5194/sp-2023-10
 - Fisheries and Oceans Canada. (2025). *Bedford Basin Monitoring Program (BBMP)*. Available at: https://www.bio.gc.ca/science/monitoring-monitorage/bbmp-pobb/bbmp-pobb-en.php (last access: 30 September 2025).
- Forster, S., Turnewitsch, R., Powilleit, M., Werk, S., Peine, F., Ziervogel, K., & Kersten, M. (2009). Thorium-234-derived information on particle residence times and sediment deposition in shallow waters of the south-western Baltic Sea. *Journal of Marine Systems*, 75(3–4), 360–370. https://doi.org/10.1016/j.jmarsys.2008.04.004
- Foster, J. M., & Shimmield, G. B. (2002). 234Th as a tracer of particle flux and POC export in the northern North Sea during a coccolithophore bloom. *Deep-Sea Research Part II: Topical Studies in Oceanography*, 49(15), 2965–2977. https://doi.org/10.1016/S0967-0645(02)00066-8
 - GEBCO Compilation Group. (2022). *GEBCO 2022 Grid* [Dataset]. https://doi.org/10.5285/c6612cbe-50b3-0cff-e053-6c86abc040b9
- Graff, J. R., Nelson, N. B., Roca-Martí, M., ... Siegel, D. A. (2023). Reconciliation of total particulate organic carbon and nitrogen measurements determined using contrasting methods in the North Pacific Ocean (NASA EXPORTS). *Elementa:*Science of the Anthropocene, 11(1), 00112. https://doi.org/10.1525/elementa.2022.00112
 - Haas, S., Robicheau, B. M., Rakshit, S., Tolman, J., Algar, C. K., LaRoche, J., & Wallace, D. W. R. (2021). Physical mixing in coastal waters controls and decouples nitrification via biomass dilution. *Proceedings of the National Academy of Sciences*, 118(18), e2004877118. https://doi.org/10.1073/pnas.2004877118
- Hargrave, B. T., Phillips, G. A., & Taguchi, S. (1976). Sedimentation measurements in Bedford Basin, 1973–74. Fish. Mar. Ser. Res. Dev. Rep. https://doi.org/10.13140/2.1.2815.3125

- Hargrave, B. T., & Taguchi, S. (1978). Origin of deposited material sedimented in a marine bay. *Journal of the Fisheries Research Board of Canada*, 35, 1604–1613. https://doi.org/10.1139/f78-250
- Hung, C.-C., Gong, G.-C., & Santschi, P. H. (2012). 234Th in different size classes of sediment-trap collected particles from the northwestern Pacific Ocean. *Geochimica et Cosmochimica Acta*, 91, 60–74. https://doi.org/10.1016/j.gca.2012.05.017
- Kepkay, P. E., Niven, S. E. H., & Jellett, J. F. (1997). Colloidal organic carbon and phytoplankton speciation during a coastal bloom. *Journal of Plankton Research*, 19(3), 369–389. https://doi.org/10.1093/plankt/19.3.369
 - Lalande, C., Moran, S. B., Wassmann, P., Grebmeier, J. M., & Cooper, L. W. (2008). 234Th-derived particulate organic carbon fluxes in the northern Barents Sea with comparison to drifting sediment trap fluxes. *Journal of Marine Systems*, 73(1–2), 103–113. https://doi.org/10.1016/j.jmarsys.2007.09.004
- Lam, P. J., Ohnemus, D. C., & Auro, M. E. (2015). Size-fractionated major particle composition and concentrations from the US GEOTRACES North Atlantic zonal transect. *Deep-Sea Research Part II: Topical Studies in Oceanography*, 116, 303–320. https://doi.org/10.1016/j.dsr2.2014.11.020
- Lepore, K., Moran, S. B., Grebmeier, J. M., Cooper, L. W., Lalande, C., Maslowski, W., Hill, V., Bates, N. R., Hansell, D. A., Mathis, J. T., & Kelly, R. P. (2007). Seasonal and interannual changes in particulate organic carbon export and deposition in the Chukchi Sea. *Journal of Geophysical Research: Oceans*, 112(C10), C10S90. https://doi.org/10.1029/2006JC003555
 - Li, W. K. W., & Dickie, P. M. (2001). Monitoring phytoplankton, bacterioplankton and virioplankton in a coastal inlet (Bedford Basin) by flow cytometry. *Cytometry*, 44(3), 236–246. https://doi.org/10.1002/1097-0320(20010701)44:3<236::AID-CYTO1116>3.0.CO;2-5
- Li, W. K. W., & Harrison, W. G. (2008). Propagation of an atmospheric climate signal to phytoplankton in a small marine basin. *Limnology and Oceanography*, 53(5), 1734–1745. https://doi.org/10.4319/lo.2008.53.5.1734
 - Lin, W., Chen, L., Zeng, S., Li, T., Wang, Y., & Yu, K. (2016). Residual β activity of particulate 234Th as a novel proxy for tracking sediment resuspension in the ocean. *Scientific Reports*, 6, 27069. https://doi.org/10.1038/srep27069
 - Longhurst, A., Sathyendranath, S., Platt, T., & Caverhill, C. (1995). An estimate of global primary production in the ocean from satellite radiometer data. *Journal of Plankton Research*, 17(6), 1245–1271. https://doi.org/10.1093/plankt/17.6.1245
- Luo, Y., Miller, L. A., De Baere, B., Soon, M., & Francois, R. (2014). POC fluxes measured by sediment traps and 234Th:238U disequilibrium in Saanich Inlet, British Columbia. *Marine Chemistry*, 162, 19–29. https://doi.org/10.1016/j.marchem.2014.03.001
 - Martin, J. H., Knauer, G. A., Karl, D. M., & Broenkow, W. W. (1987). VERTEX: Carbon cycling in the northeast Pacific. *Deep-Sea Research Part A: Oceanographic Research Papers*, 34(2), 267–285. https://doi.org/10.1016/0198-0149(87)90086-0
- Muller-Karger, F. E., Varela, R., Thunell, R., Luerssen, R., Hu, C., & Walsh, J. J. (2005). The importance of continental margins in the global carbon cycle. *Geophysical Research Letters*, 32(1), L01602. https://doi.org/10.1029/2004GL021346
 - Niven, S. E. H., Kepkay, P. E., & Boraie, A. (1995). Colloidal organic carbon and colloidal 234Th dynamics during a coastal phytoplankton bloom. *Deep-Sea Research Part II: Topical Studies in Oceanography*, 42(1), 257–273. https://doi.org/10.1016/0967-0645(95)00014-H
- Owens, S. A., Buesseler, K. O., & Sims, K. W. W. (2011). Re-evaluating the 238U–salinity relationship in seawater: Implications for the 238U–234Th disequilibrium method. *Marine Chemistry*, 127(1–4), 31–39. https://doi.org/10.1016/j.marchem.2011.07.005
 - Owens, S. A., Pike, S., & Buesseler, K. O. (2015). Thorium-234 as a tracer of particle dynamics and upper-ocean export in the Atlantic Ocean. *Deep-Sea Research Part II: Topical Studies in Oceanography*, 116, 42–59.
- 740 https://doi.org/10.1016/j.dsr2.2014.11.010

- Pike, S. M., Buesseler, K. O., Andrews, J., & Savoye, N. (2005). Quantification of 234Th recovery in small-volume seawater samples by inductively coupled plasma mass spectrometry. *Journal of Radioanalytical and Nuclear Chemistry*, 263(2), 355–360. https://doi.org/10.1007/s10967-005-0594-z
- Platt, T. (1975). Analysis of the importance of spatial and temporal heterogeneity in the estimation of annual production by phytoplankton in a small, enriched, marine basin. *Journal of Experimental Marine Biology and Ecology*, 18, 99–109.
 - Puigcorbé, V., Masqué, P., & Le Moigne, F. A. C. (2020). Global database of ratios of particulate organic carbon to thorium-234 in the ocean: Improving estimates of the biological carbon pump. *Earth System Science Data*, 12(2), 1267–1287. https://doi.org/10.5194/essd-12-1267-2020
- Rakshit, S., Dale, A. W., Wallace, D. W., & Algar, C. K. (2023). Sources and sinks of bottom-water oxygen in a seasonally hypoxic fjord. *Frontiers in Marine Science*, 10, 1148091. https://doi.org/10.3389/fmars.2023.1148091
 - Rakshit, S., Glock, N., Dale, A. W., ... Algar, C. K. (2025). Foraminiferal denitrification and deep bioirrigation influence benthic biogeochemical cycling in a seasonally hypoxic fjord. *Geochimica et Cosmochimica Acta*, 388, 268–282. https://doi.org/10.1016/j.gca.2024.10.010
- Robicheau, B. M., Tolman, J., Bertrand, E. M., & LaRoche, J. (2022). Highly resolved interannual phytoplankton community dynamics of the coastal Northwest Atlantic. *ISME Communications*, 2(1), 38. https://doi.org/10.1038/s43705-022-00119-2
 - Shan, S., & Sheng, J. (2012). Examination of circulation, flushing time and dispersion in Halifax Harbour of Nova Scotia. *Water Quality Research Journal*, 47(3–4), 353–374. https://doi.org/10.2166/wqrjc.2012.041
 - Shan, S., Sheng, J., Thompson, K. R., & Greenberg, D. A. (2011). Simulating the three-dimensional circulation and hydrography of Halifax Harbour using a multi-nested coastal ocean circulation model. *Ocean Dynamics*, 61(7), 951–976. https://doi.org/10.1007/s10236-011-0398-3
 - Shi, Q., & Wallace, D. (2018). A three-year time series of volatile organic iodocarbons in Bedford Basin, Nova Scotia: A northwestern Atlantic fjord. *Ocean Science*, 14(6), 1385–1403. https://doi.org/10.5194/os-14-1385-2018

- Siegel, D. A., Buesseler, K. O., Doney, S. C., Sailley, S. F., Behrenfeld, M. J., & Boyd, P. W. (2014). Global assessment of ocean carbon export by combining satellite observations and food-web models. *Global Biogeochemical Cycles*, 28(3), 181–196. https://doi.org/10.1002/2013GB004743
 - Trimble, S. M., & Baskaran, M. (2005). The role of suspended particulate matter in 234Th scavenging and 234Th-derived export fluxes of POC in the Canada Basin of the Arctic Ocean. *Marine Chemistry*, 96(1–2), 1–19. https://doi.org/10.1016/j.marchem.2004.10.003
- Turnewitsch, R., & Springer, B. M. (2001). Do bottom mixed layers influence 234Th dynamics in the abyssal near-bottom water column? *Deep-Sea Research Part I: Oceanographic Research Papers*, 48(2), 239–257.
 - Wassmann, P. (1984). Sedimentation and benthic mineralization of organic detritus in a Norwegian fjord. *Marine Biology*, 83(1), 83–94. https://doi.org/10.1007/BF00393088
 - Wei, C.-L., & Murray, J. W. (1992). Temporal variations of 234Th activity in the water column of Dabob Bay: Particle scavenging. *Limnology and Oceanography*, 37(2), 296–314. https://doi.org/10.4319/lo.1992.37.2.0296
- Yang, W., Tian, J., Chen, M., Zheng, M., & Chen, M. (2022). A new radiotracer for particulate carbon dynamics: Examination of 210Bi–210Pb in seawater. *Geochemistry, Geophysics, Geosystems*, 23(12), e2022GC010656. https://doi.org/10.1029/2022GC010656
- Ziervogel, K., Sweet, J., Juhl, A. R., & Passow, U. (2021). Sediment resuspension and associated extracellular enzyme activities measured ex situ: A mechanism for benthic–pelagic coupling in the deep Gulf of Mexico. *Frontiers in Marine Science*, 8, 668621. https://doi.org/10.3389/fmars.2021.668621